

Doctoral Thesis Summary

Applied Rheology for Production of Polymeric Nanofibers

Aplikovaná reologie pro výrobu polymerních nanovláken

Author: **Ing. Bc. Jiří Drábek, Ph.D.**

Degree programme: P2808 Chemistry and Materials Technology

Degree course: 2808V006 Technology of Macromolecular Compounds

Supervisor: prof. Ing. Martin Zatloukal, Ph.D., DSc.

Reviewers: prof. Ing. Kamil Wichterle, DrSc., dr. h. c.
prof. Ing. Ivan Chodák, DrSc.
prof. Ing. Pavel Alexy, Ph.D.

Zlín, December 2018

© Ing. Bc. Jiří Drábek, Ph.D.

Published by **Tomas Bata University in Zlín** in the Edition **Doctoral Thesis Summary**.

The publication was issued in the year 2018

Keywords in English: *Melt blown technology, Polymeric nanofibers, Polypropylene, Constitutive equations, Thermal degradation, High shear rate rheology, Extensional rheology*

Keywords in Czech: *Technologie melt blown, Polymerní nanovlákná, Polypropylen, Konstituční rovnice, Termální degradace, Smyková reologie, Elongační reologie*

Full text of the doctoral thesis is available in the Library of TBU in Zlín.

ISBN 978-80-7454-819-2

ACKNOWLEDGEMENT

I would like to express my sincere gratitude to all people who supported me during the study and work on this thesis.

I am especially grateful to my supervisor, prof. Ing. Martin Zatloukal, Ph.D., DSc. for his patience, valuable advices, support throughout the process of measuring and analyzing data and writing the thesis.

Many thanks go to Joachim Fiebig for his support during measurements on the melt blown pilot plant line during my research stay in BOREALIS Company, Linz, Austria.

My acknowledgement also belongs to Mike T. Martyn from University in Bradford, United Kingdom, for his advices during my experiment on Fanuc Roboshot S-2000i 100A.

I would like to express my thanks to my colleague Tomas Barborik for his assistance, whenever I applied for it.

I also wish to acknowledge Grant Agency of the Czech Republic (Grant registration No. 16-05886S) for the financial support.

I would like to extend my gratitude to my family and all my real friends for their support and patience during my study.

ABSTRACT

The first part of this work summarizes the current state of knowledge in area of melt blown technology, which allows production of polymeric nanofibers, with specific attention to the most commonly utilized polymers (including linear and branched polypropylenes), description of methodologies to produce nanofibers, the role of processing conditions on produced fibers, related flow instabilities and high shear rate rheology. In the second part of this work, chosen polymers, methodologies and instruments are provided in order to understand complicated relationship between polymer melt rheology, their molecular structure, process conditions and formation of polymeric fibers produced via melt blown technology. For such purpose, different polypropylenes (PPs) (namely linear, branched and their blends) having well defined molecular architecture were chosen and rheologically characterized in very wide shear rate range utilizing advanced constitutive equations. Then, the chosen PPs were used to produce polymeric fibers on the melt blown pilot plant line under different processing conditions in order to perform particular correlations. It has been found that the melt strength of branched PP can increase at short degradation times due to, presumably, creation of a high number of short branches, even if the molecular weight decreased due to chain scission. For the first time, it has been discovered that the secondary Newtonian viscosity (occurring above shear rates of $2 \times 10^6 \text{ s}^{-1}$), depends linearly on the average molecular weight, which suggests that polymer chains are fully disentangled at the secondary Newtonian plateau region. It was found that introduction of long-chain branching into PP, keeping the average molecular weight and polydispersity index the same, can firstly, decrease the secondary Newtonian plateau, which can primarily be attributed to smaller coils size and higher availability of the free volume for the branched PP in comparison with pure linear PP melt and secondly, it stabilizes melt blown process due to increased elasticity. Obtained scientific knowledge can help to understand production of polymeric nanofibers and its optimization considerably.

Keywords: Melt blown technology • Polymeric nanofibers • Polypropylene • Constitutive equations • Thermal degradation • High shear rate rheology • Extensional rheology

ABSTRAKT

První část předložené práce shrnuje současný stav poznání v oblasti melt blown technologie umožňující produkci polymerních nanovláken se specifickým důrazem na nejčastěji používané polymery, popis metodik pro produkci nanovláken, roli procesních podmínek, typické tokové nestability a reologické chování polymerních tavenin při vysokých smykových rychlostech. Druhá část práce pak sumarizuje použité polymery, metodiky a experimentální zařízení, které byly použity pro porozumění komplikovaných vztahů mezi reologickým chováním polymerů, jejich molekulární strukturou, procesními podmínkami a tvorbou vláken pomocí technologie melt blown. Pro tento účel byly použity různé typy polypropylenů (lineární, rozvětvené a jejich blendy) s dobře definovanou molekulární strukturou, které byly reologicky charakterizovány ve velmi širokém rozsahu deformačních rychlostí s využitím pokročilých konstitutivních rovnic. Vybrané polypropyleny byly následně použity k produkci vláken na výrobní melt blown lince za různých procesních podmínek s cílem provést dané korelace. Bylo zjištěno, že pevnost taveniny rozvětveného PP může při krátkých degradačních časech růst (pravděpodobně díky vzniku vysokého počtu krátkých větví), a to i přesto, že jeho molekulová váha, v důsledku štěpení jednotlivých řetězců, klesá. Poprvé bylo objeveno, že smyková viskozita tavenin PP je v oblasti druhého Newtonského plató (tj. při deformačních rychlostech vyšších než $2 \times 10^6 \text{ s}^{-1}$) lineárně závislá na molekulové hmotnosti, což svědčí o celkovém rozpletení jednotlivých řetězců. Bylo objeveno, že při zavedení bočních větví do PP (při zachování jeho molekulové hmotnosti a stupně polydisperzity) dochází k poklesu jeho viskozity v oblasti druhého Newtonského plató, růstu elasticity a stabilizaci produkce vláken pomocí technologie melt blown (jako přímý důsledek poklesu gyračního poloměru makromolekulárních klubek a zvýšení dostupnosti volného objemu mezi nimi). Získané vědecké poznatky mohou výrazně přispět k porozumění a optimalizaci výroby polymerních nanovláken.

Klíčová slova: Technologie melt blown • Polymerní nanovlákná • Polypropylen • Konstituční rovnice • Termální degradace • Smyková reologie • Elongační reologie

CONTENT

LIST OF PAPERS	7
1. MELT BLOWN	8
1.1 Melt blown history	8
1.2 Melt blown definition	10
1.3 Melt blown webs	14
1.3.1 Melt blown nanofibers	17
1.3.2 Processing conditions	19
1.4 Flow instabilities and defects in melt blown technology	22
2. POLYPROPYLENE	28
2.1 Linear polypropylene	28
2.2 Branched polypropylene	29
3. HIGH SHEAR RHEOLOGY	32
THE AIMS OF THE DOCTORAL RESEARCH WORK	35
4. MATERIALS AND INSTRUMENTS	36
4.1 Rotational Rheometer (ARES 2000)	36
4.2 Extensional Rheometer (SER-HV-A01)	38
4.3 Capillary Rheometer (Rosand RH7-2)	39
4.4 Fanuc Roboshot S-2000i 100A	40
4.5 Reifenhäuser REICOFIL pilot melt blown line	43
4.6 HITACHI Tabletop TM-1000 SEM microscope	44
SUMMARIZATION OF THE SELECTED RESEARCH RESULTS	45
THE THESIS CONTRIBUTION TO SCIENCE AND PRACTICE	56
CONCLUSION	57
REFERENCES	59
LIST OF FIGURES	75
LIST OF TABLES	77
LIST OF PUBLICATIONS	78
CURRICULUM VITAE	80

LIST OF PAPERS

The following papers are included in the present doctoral thesis:

PAPER I

Evaluation of Thermally Induced Degradation of Branched Polypropylene by Using Rheology and Different Constitutive Equations

Jiri Drabek, Martin Zatloukal

Polymers, 2016, vol. 8, no. 9, article number 317.

PAPER II

Effect of Molecular Weight on Secondary Newtonian Plateau at High Shear Rates for Linear Isotactic Melt Blown Polypropylenes

Jiri Drabek, Martin Zatloukal, Mike Martyn

Journal of Non-Newtonian Fluid Mechanics, 2018, vol. 251, pp. 107-118.

PAPER III

Effect of Molecular Weight, Branching and Temperature on Dynamics of Polypropylene Melts at Very High Shear Rates

Jiri Drabek, Martin Zatloukal, Mike Martyn

Polymer, 2018, vol. 144, pp. 179-183

PAPER IV

Influence of Long Chain Branching on Fiber Diameter Distribution for Polypropylene Nonwovens

Jiri Drabek, Martin Zatloukal

Submitted for publication in *Journal of Rheology*, 2018

1. MELT BLOWN

1.1 Melt blown history

Carlton Francis was the first person who tried to develop microfibers. In 1939 he pictured a spray gun which was to create textile like microfibers. Since 1940's to mid. 1960's three companies (American Viscose, Dow Chemical Company and Chemstrand Company) were trying to develop microfibers by using a spray spinning technique. However, none company achieved their expected results. For that reason, all three companies discontinued research on the projects. In the early 1950's, melt blown (MB) technology was developed under the United States Army Chemical Warfare Laboratories based on the previous Dow's research on production of microfibers [1]. In 1954, Van A. Wenté together with his colleagues were the first, who demonstrated the concept of melt blowing process that formed microfibers or fibers less than 10 microns in diameter from thermoplastic polymers. Wenté et al. conducted their research at the United States Naval Research Laboratory to develop microfibers in order to produce filters on drone aircraft used to monitor radiation from US and Russian nuclear tests [2]. During the 1960's, Esso Research and Engineering Company (now ExxonMobil Corporation) followed the Wenté's work and they were able to improve and scale up the line (from 3 to 40 inches die width) the process considerably to successfully produce low-cost PP microfibers [1]. The original naval development work by Wenté achieved production rates of only $1.5 \times 10^{-4} - 4.5 \times 10^{-4}$ kg/s/m of die width whereas Esso was able to improve the technology to commercial attractive throughput levels of $6.5 \times 10^{-3} - 12.9 \times 10^{-3}$ kg/s/m of die width [3]. Furthermore, they improved Wenté's die design to minimize flaws known as "shots" [1]. The initial development was oriented for battery separators and synthetic electrical paper. Esso developed a 3-ply calendered PP laminate for this application [4]. By the mid-1960's, the process and technology was patented by Esso and coined the "Meltblown Process" [1]. Esso's affiliate in Japan retained the right to commercialize the technology and did so quite successfully by producing and marketing Tapyrus MB products and become one on the earliest commercial melt blowing process practitioners. Thus, Esso became the first to demonstrate, patent, publicize and license the use of the Wenté concept as a very practical one-step process to produce unique types of nonwoven webs, tow, bats, etc. [2]. In the 1970's, Esso recognized potential use in filtration, hygiene products, adhesive webs, cigarette filters and specialty synthetic papers. They also recognized the possibilities of combining MB webs with other webs, especially for

reinforcement, through laminations and coatings. Esso built an extensive patent position for MB [4]. They licensed the process out to companies which included Kimberley-Clark, Johnson & Johnson, James River, Web Dynamics, Ergon Nonwoven, Riegel, and Dewey & Almy so they could focus more on developing and producing the resin for the MB process [1]. From 1970 to 2000, over 320 U.S. patents have been granted to the technologies and products related to melt blowing. Only 20 patents were granted in the 70's; it increased to 64 patents in the 80's and jumped to 236 patents in the 90's. It is clear that the MB technology is finding its application in more and more fields [5]. Development of publication activity about nanofibers from the 70's until August 2018 is displayed in Figure 1. In 1983, Esso teamed with the University of Tennessee, Knoxville and built the first pilot line to ensure ongoing research for technological advancements in the MB process [1].

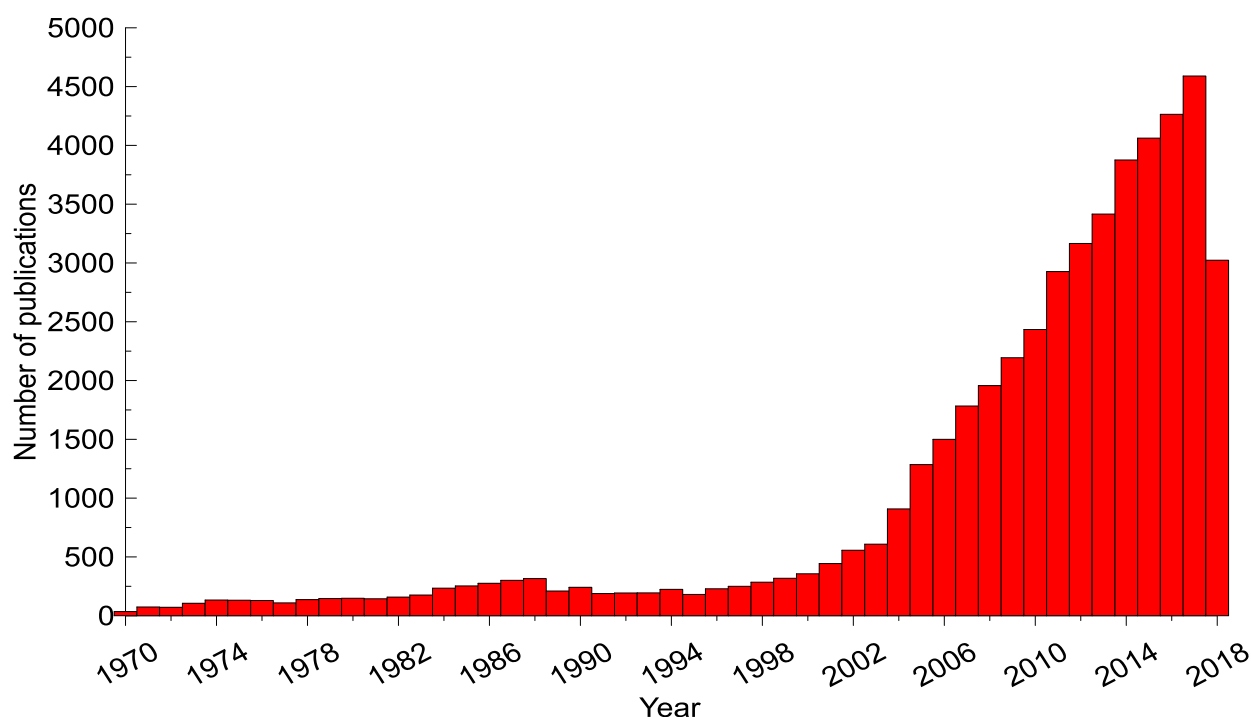


*Fig. 1: Development of publication activity about nanofibers [6]
(data taken in August 2018)*

1.2 Melt blown definition

Melt blowing, as shown in Figure 2, is a simple, versatile and one step process for the convert polymeric raw materials into nonwovens. MB process includes five constituents that are the extruder, metering pump, die assembly, web formation and winding [1, 7]. The polymer in the form of pellets, granules, powder or chips is gravity-fed from hopper to the extruder at a certain feed rate [7]. In the extruder, polymer is going through three zones (feed zone, transition zone, exit zone). After passage through zones, the polymer becomes a polymer melt. Then the polymer melt is transferred into the metering zone.

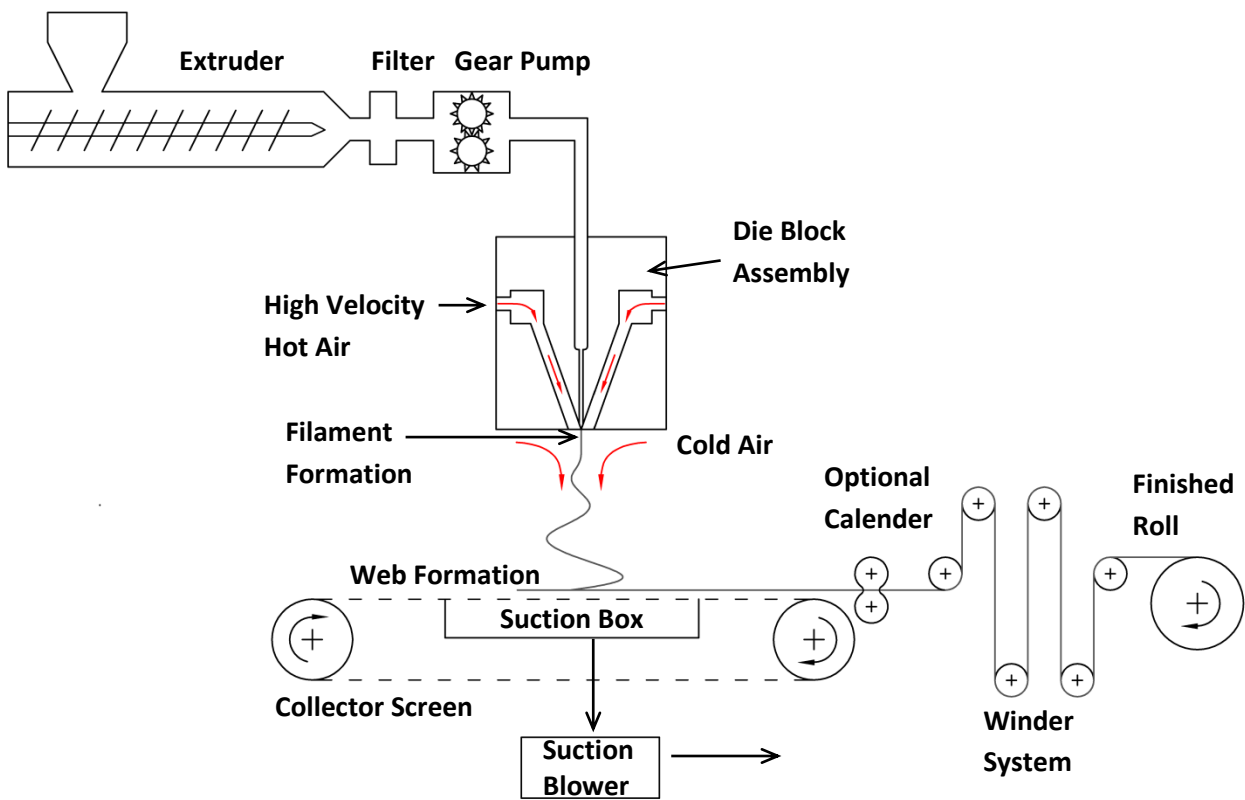


Fig. 2: Scheme of MB line [1, 8]

Metering pump, known also as gear pump delivers the polymer melt uniformly and consistently to the die assembly. Die assembly is the most important and unique part of the MB system and is responsible for the quality of the produced fibers [1, 7]. A die assembly consists of a polymer feed distribution system, such as a Coat-hanger, T-die or Fishtail die, to provide even polymer flow and residence time across the width of the MB die, a nose tip which could be also several types with different designs, and air manifolds [1]. An air assembly

provides air streams with different temperatures reaching typically 50 – 80 % of sound speed [1]. A polymer melt is extruded through small orifices into convergent streams of hot air [9, 10]. The drag force of the air causes rapid melt elongation into a fine fiber with a small diameter [9, 10], as it is depicted in Figure 3. It was reported that the highest fiber diameter reduction occurs at very small post die distances (typically between 10 and 20 mm) and very short times (0.05 ms) [11, 12]. During fiber attenuation, very high extensional strain rates ($\sim 10^6 \text{ s}^{-1}$) are achieved [13]. The air streams, having typically the same temperature like polymer melt, also help to transport fibers to a collector [9]. Collector is picking up the attenuated filament streams, which leads to a nonwoven web formation with an almost random network of fibers [1]. At the end, the nonwoven web is wound into a cylindrical package for easier subsequent handling [1, 5 – 13].

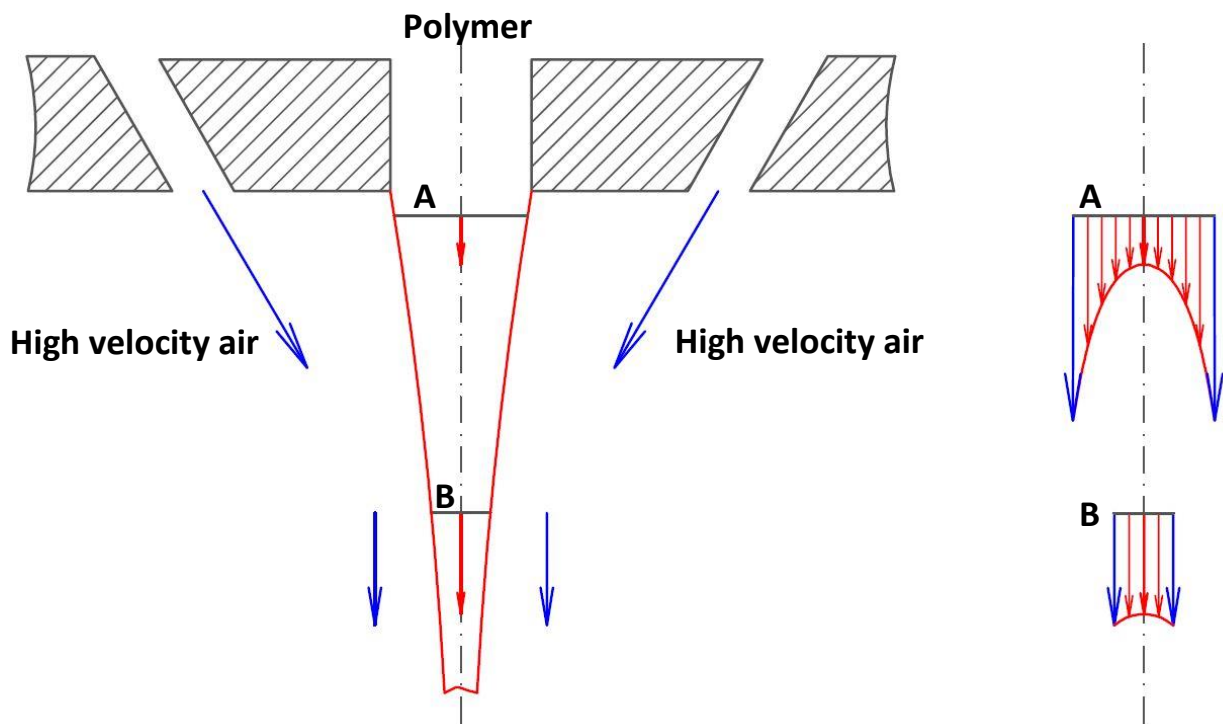


Fig. 3: Visualization of fiber attenuation in post die area during MB process (left) together with particular velocity profiles in cross sections A and B (right) [14]

Table 1 and Figure 4 summarize development in MB die design in chronological order.

Table 1. Summarization of the most important MB die designs in chronological order [5, 15, 16]

Publication date	Identification number	Title	Inventor/author	Description	Notation in Fig. 4
23. 7. 1974	US-3825379-A	Melt-blowing die using capillary tubes	D. Lohkamp, J. Keller	The die is a two-piece assembly and capillary tubes are included in the solder layer between the two pieces to form the die apparatus. Capillary type has the advantages in achieving longer holes and more precise alignment of the orifice with great ease.	A
23. 7. 1974	US-3825380-A	Melt-blowing die for producing nonwoven mats	J. Harding, J. Keller, R. Buntin	Drilled hole type MB die, which usually has a pair of air slots in each side of the nosepiece, that are connected to the air manifolds and can be adjusted to form different die settings.	B
19. 4. 1983	US-4380570-A	Apparatus and process for melt-blowing a fiber forming thermoplastic polymer and product produced thereby	Eckhard C. A. Schwarz	Fiber-forming polymer is heated up to low viscosity and accelerated quickly by nozzle blown air to near sonic velocity to produce fine fibers with little polymer degradation. This discovery broke the limitation of air from two sides of the tapered die tip. Therefore, a number of orifice rows can be arrayed in a single die head to achieve desirable productivity without tremendous capital increase.	C
19. 1. 1988	US-4720252-A	Slotted melt-blown die head	D. W. Appel, A. D. Drost, J. C. Lau	The slot die has a single continuous slot opening running its length, instead of a number of individual orifices. In order to produce fiber instead of film, at least one of the inner sides of the slot has spaced grooves perpendicular to the apex line and one of the sides extends below the other side to form a lip within the fluid stream.	D
22. 1. 1991	US-4986743-A	Melt blowing die	P. G. Buchning	The die tip is mounted by bolting inwardly toward the orifices onto the die body. Opposite and equal forces are applied on both sides of the orifice row to secure the die tip. The mounted die tip can be then easily disassembled and cleaned by specialty techniques and equipment, such as high temperature ovens and ultrasonic cleaners.	E
8. 4. 1997	US-5618566-A	Modular meltblowing die	M. A. Allen, J. T. Fetcko	Modular dies enables the users to vary the length of the die by merely adding modules or removing modules from structure. Each module consists of a body, a die tip assembly, and polymer and air flow passages for conducting hot melt and hot air from the manifold through each module. The cost of modular die tip is approximately \$300/inch, which is relatively inexpensive comparing to \$1300/inch for regular single-row-orifice, single-metal long die tip.	F
8. 8. 2000	US-6099282-A	Multihole melt blown die nosepiece	M. W. Milligan	MB die nosepiece comprises a multiplicity of offset holes for hot melt extrusion. In each pair of adjacent holes, the first hole angled toward the upper face and a second hole angled toward the lower face. It is claimed that this nosepiece reduces the filament-to-filament interaction, thus minimizing the "shot" formation.	G
19. 12. 2006	US-7150616-B2	Die for producing meltblown multicomponent fibers and meltblown nonwoven fabrics	B. D. Haynes, M. Ch. Cook	A die tip adapted for extruding a plurality of melt blown multicomponent filaments that includes at least two series of conduits that extend and converge in to the interior of the die tip to convey a multicomponent thermoplastic structure in to the interior of the die tip to a series of capillaries that extend to a series of die opening for extruding multicomponent filaments is provided.	H
31. 1. 2008	US-2008023888-A1	Method and apparatus for production of meltblown nanofibers	J. Brang, A. Wilkie, J. Haggard	A MB spinneret die having spin holes formed by grooves in plate(s) surface(s) of plate(s) where polymer exits at the plate(s) edge(s). The grooves are 0.127 mm in wide and 0.102 mm deep or smaller. The spin hole L/D ratios are 20/1 or greater, preferably as high as 200/1 or even 1000/1. Spin holes are arranged in linear arrays with a density of 99 or even 199 holes per inch.	I
9. 3. 2017	US-2017067184-A1	Melt blowing die, apparatus and method	M. A. Allen	A melt blowing die includes a stack of plates including corresponding melt blowing die tip, die body and air functionalities. The stack may include at least 20-60 plates per centimeter of length and 1-20 rows of orifices.	J
16. 11. 2017	JP-2017203233-A	Melt-blowing die	H. Adachi, Y. Miura	MB die is special by two air channels: a primary air flow passage which is provided such that the resin flow passage is interposed therein, and which blows primary air downward against the molten resin discharged through the resin flow passage; and a secondary air flow passage which is provided such that the primary air flow passage is interposed therein, and which blows secondary air from the outside of the primary air.	K

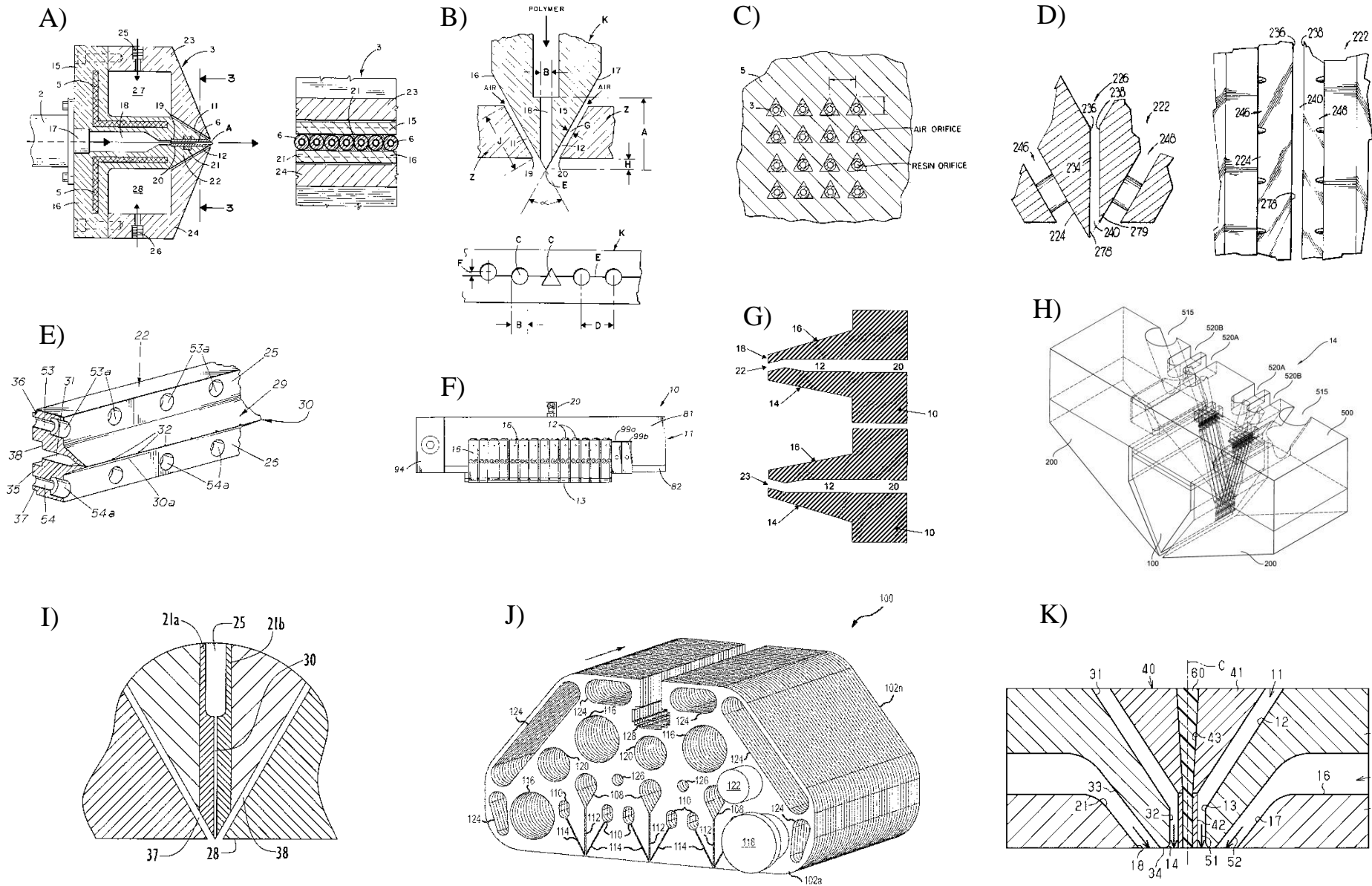


Fig. 4: Summarization of the MB die designs described in Table 1

1.3 Melt blown webs

MB fabric properties can be tuned depending on end-use requirements by adjusting polymer section, process conditions, bonding and finishing processes. Basic characteristics and properties of MB webs are [17]:

- Random fiber orientation.
- Low to moderate web strength.
- Generally, the web is highly opaque (high cover factor).
- MB webs derive their strength from mechanical entanglement and frictional forces.
- Most MB webs are layered or shingled structure, the number of layers increases with increasing basis weight.
- Fiber diameter ranges between 0.5 and 30 μm , but the typical range is 2 to 7 μm (or 1 to 2 μm [3]).
- Basis weight ranges between 8 and 350 g/m^2 , typically 20 – 200 g/m^2 .
- Microfibers provide high surface areas for good insulator and filter characteristics.
- The fibers have a smooth surface texture and appear to be circular in cross-section.
- The fibers vary in diameter along a single fiber.
- Close examination of approximately 800 photomicrographs showed no ‘fibre-ends’ (except a few near areas where ‘shot’ is present), therefore, the fibers are believed to be mostly continuous in length.

Melt blowing process is highly versatile in respect of the range of polymers that can be processed. PP is the most widely used resin in melt blowing due to its ease of processing and suitability for end-use. PP accounts for 70 % of the spunlaid resins used to manufacture nonwovens in North America. A typical PP used for melt blowing would have an MFR between 30 – 1,500 g/10 minutes [17]. However, there are many thermoplastic polymers used in the MB process although some of them are more commonly used than others. The polymers which are summarized in Table 2 have been used for production of nonwovens via MB technology. Blends of different polymer types and configurations are now tailored towards the end-user’s requirements. Also there are several additives incorporated during the resin manufacturing process to supply various grades of the same polymer with large differences in their melt flow rates [1, 4, 17 – 19].

Table 2. Typical polymers utilized in the MB technology [1, 20]

Common	Others
Polypropylene (PP)	Ethylene vinyl acetate (EVA)
Polystyrene (PS)	Ethylene methacrylate (EMA)
Polyesters	Ethylene vinyl alcohol (EVOH)
Polyurethane (PUR)	Fusibles of copolymers
Polyamide (PA 6, 66, 11, 12)	Polybutylene terephthalate (PBT)
Polyethylene (PE)	Polyphenylene sulfide (PPS)
Low and high density polyethylene (LDPE, HDPE)	Polymethylpentene (PMP)
Linear low-density polyethylene (LLDPE)	Polyvinyl alcohol (PVA)
Polycarbonate (PC)	Polyethylene sulfide
	Fluoropolymers
	Polytrifluorochloroethene (PCTFE)
	Polyethylene terephthalate (PET)
	Poly (4-methylpent-1-ene)
	Polytetramethylene Terephthalate (PTMT)
	Sulfopolyester
	Polyvinylidene fluoride (PVDF)

Production of nonwovens began more than two decades ago, the industry remains to be the fastest growing sectors of textile materials in the world. Worldwide production grew from about 2.6 million tons in 1996, worth about \$10 billion, to around 8.9 million tons in 2014, worth \$35.6 billion, and is predicted to reach to 12.4 million tons by 2020 [20]. As the nonwoven market continues to expand, the introduction of biodegradable, sustainable raw products to create nonwovens remains unchanged. Nonwovens exhibit specific features such as strength, elongation, resilience, liquid repellency, softness, washability, filtering capacity, bacteria barrier, and sterility. Among the various applications, many of the products are classified as disposable products which account for nearly two-thirds the demand of nonwoven fabrics [19, 20]. The most typical MB products, together with their application fields, are provided in Table 3.

Table 3. Summarization of products, which can be produced by the MB technology [1] (adapted from [21])

Field of applications	Products
Filtration	HVCA filter, HEPA filter, ULPA filter, oil filter, respiratory filter, teabags, vacuum cleaner filter bags, dry and liquid aerosol filter, odour control, activated carbon filter, liquid filters.
Medical	Surgical gowns, face masks, drapes, caps, bandages, tapes, wound dressings, pads, sponges, cover stocks, sterile packaging, heat pack.
Sorbents & Wipes	Household wipes, industrial clean up wipes, oil clean up (oil booms), food fat absorption
Hygiene	Baby diapers, feminine sanitary napkins, adult incontinence pads, tampons, nasal trips.
Industrial	Absorbent, lubricating pads, papermaking felts, conveyor belts, packaging, artificial leathers, battery separator, abrasives.
Automobiles	Side, front and back liner, floor mat, sheet cover, wheelhouse cover, oil filter, engine air filter, sounds absorbing panel.
Agriculture	Root bags, weed control fabric, water retention fabric, crop cover or seed protector, soil separation, capillary mat, containers.
Geotextiles	Pond and river liner for erosion control, soil stabilization, road bed, drainage.
Construction and civil engineering	Insulation nonwoven, pipe wrap, insulation ceilings or false ceiling, house wrap, shingle.
Household	Cushion covers, blankets, bed sheets, quilt back, pillow covers, curtains, envelopes, aprons, dust cloth, CD case, wall paper, carpet backings, bags.
Clothing	Interlinings, pads, disposable underwear, shoe, belt and bag components, labels, handkerchiefs, towels, dust removal cloths.
Protection	Fire protection fabrics, gas and chemical protection fabrics, thermal insulating gloves, lab coats, ballistics armour, bullet proof vest.
Transportation	Air bag, sun shade fabrics, car roof, silencer.
Electronics	Cable insulation, semiconductor polishing pad, insulating tape, battery separators.
Other	Hot-melt adhesives, apparel thermal insulator, acoustic insulation.

MB technology is also utilized in area of battery separators [4, 22], oil sorbents [23], bone tissue engineering [24] and filtration [25 – 27].

It is useful to compare MB technology to other nonwoven processes that directly produce fibrous web structure. Spunbond and melt blown webs are often combined at the production stage to achieve a variety of composite structures for protective applications particularly in the hygiene and medical sectors. In the Spunbond-Melt blown-Spunbond (SMS) composite structure, the spunbond fabric provides the strength and the abrasion resistance and the MB

component provides the liquid and particular barrier. The SMS structure is displayed in Figure 5. Combining these two media has become a common practice in spunbond manufacturing and is finding rapidly acceptance and integration in a variety of products. There are a variety of spunbond-melt blown structural combinations available, such as Spunbond-Melt blown-Spunbond (SMS), Spunbond-Melt blown-Melt blown-Spunbond (SMMS), Spunbond-Spunbond-Melt blown-Melt blown-Spunbond (SSMMS) and others depending on the desirable final products properties [17, 28].

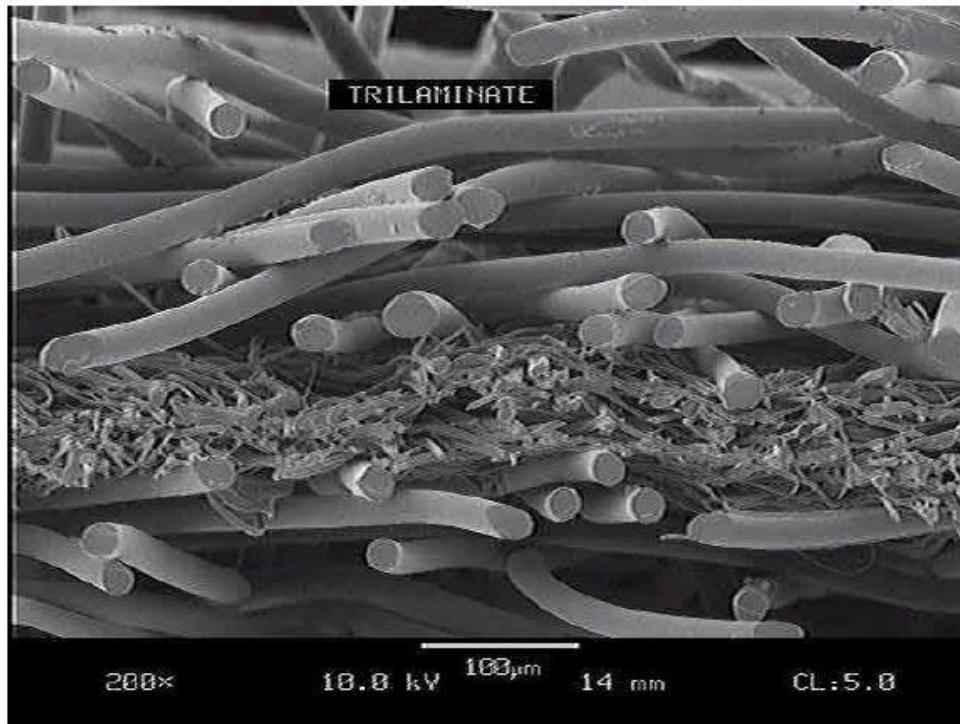


Fig. 5: Spunbond-melt blown-spunbond structure [28]

1.3.1 Melt blown nanofibers

It has been reported that polymeric nanofibers can also be produced by MB technology through, firstly, changing of processing conditions [29], secondly, by the polymer modification [30 – 32], and finally, by utilizing of special die where orifice diameters, D , are very small (0.064 – 0.127 mm) and length to diameter ratio, L/D , is very large (20/1 – 1,000/1) [15, 27, 33, 34]. In more detail, Ellison et al. [29] produced average fiber diameter less than 500 nm for PBT, PP and PS by reduced throughput and increased air flow rate. Nayak et al. [30] produced PP nanowebs (diameter of 438 – 755 nm) by lowering molecular weight of PPs (100 – 300 melt flow index, MFI) by the injection of air and water

at the vent port of the extruder. Recently, Macosko and his team showed that melt blowing immiscible polymer blends containing spherical domains can be used to produce a hierarchical nanofibers-in-microstructure from which nanofibers can be obtained by extraction of the polymer matrix with an appropriate solvent [20, 31, 32]. In more detail, Zuo F. et al. [31] has shown that it is possible to produce PBT and PECTFE nanofibers, with average diameters as small as 70 nm from MB fiber-in-fiber polymer blends. Wang Z. et al. [32] prepared nanofibers from water-extractable immiscible polymer blends containing a commercial sulfopolyester (95 %) and poly(butylene terephthalate) (5 %) with average diameter of 66 nm after washing. Soltani and Macosko [20] produced nanofibers with a record low average fiber diameter of 36 nm by islands-in-the-sea method utilizing low viscosity polymers with relatively low surface energy (i.e. having low tendency for coalescence). A special stacked plate die design with an orifice of 0.064 mm diameter was used to fabricate nanofibres with average diameter of 320 – 470 nm for a wide range of melt flow index PPs (35 – 1,200 MFI) [15]. Brang J. et al. [33] fabricated nanofibres (average fiber diameter for most of the fibres less than 500 nm) from PP, PET, PA, PE, PLA, Co-PA, PFE by melt blowing using a modified die with plate edge profile having very large length to diameter ratio ($L/D = 20/1, 200/1$ or even $1,000/1$) to achieve high web uniformity and small orifice diameters ($D = 0.12$ mm). Hassan M. A. et al. [27] manufactured nonwoven membranes by using three different die designs L/D ratio (30, 50, 200), orifice diameter (0.3048 mm, 0.1778 mm, 0.127 mm) and hole density (14, 30, 39 holes/cm). Nanofibers which were produced by these three dies have an average fiber size in the range of 300 – 500 nm. Hills Inc. (West Melbourne) produced MB nanowebs from low viscosity homopolymers (1,500 – 1,800 MFI) with average diameter of 250 nm and a range between 25 and 400 nm. According to Hills, apart from the low viscosity, smaller diameter orifices, high spin hole density (100 holes per inch) and extremely high length to diameter ratios enable the production of these nanofibers at reasonable rates, and put MB production in the same size range that was previously the exclusive domain of electrospinning technology [31, 34 – 36].

1.3.2 Processing conditions

Table 4. Effect of MB process variables on mean fiber diameter (adapted from [1] and upgraded based on the recent open literature)

Principle Investigator	Researchers	Dependent Variable	Independent Variables										
		Mean Fiber Diameter	Polymer Throughput	Polymer Temp.	MFI	Air Flow Rate	Air Velocity	Air Pressure	Air Temp.	Die Temp.	Die to collector distance (DCD)	Others	
	Chen, Li, & Huang (2005a) [37]	↓	↓	-	-	-	↑	-	-	-	↑	-	
	Chen, Wang, & Huang (2005) [38]	↓	↓	↑	↑*	-	↑	-	n/a*	-	-	-	
	Chen & Huang (2004) [39]	↓	-	-	-	-	↑	-	-	-	-	-	
	Chen & Huang (2003) [40]	↓	↓	↑	-	-	↑	-	↑	-	-	↓ angle between the slot and the spinneret axis ↓ die head width ↑ slot width	
	Chen, Wang, & Huang (2004) [41]	↓	-	-	-	-	-	-	-	-	-	↓ angle between the slot and the spinneret axis ↓ die head width ↑ slot width	
	Wu, Huang & Chen (2014) [42]	↓	↓	-	-	-	↑	-	-	-	-	-	
Bresee	Bresee & Qureshi (2006) [43]	↓↑	↑	-	-	↑	-	-	-	↑	↑	Collector speed n/a	
Shambaugh	Kaysner & Shambaugh (1990) [44]	↑↓	↑	-	-	-	-	-	-	-	-	Capillary diameter (d_1) ↑ Annulus orifice diameter (d_2) ↓ Nozzle dimensions (A_s/A_f) ↓	
	Uyttendaele & Shambaugh (1990) [45]	↓	-	-	-	-	-	-	-	-	↑	-	
	Rao & Shambaugh (1993) [11]	↓	↓	↑	-	-	↑	-	↑	-	-	-	
	Tyagi & Shambaugh (1995) [46]	↑↓	↑	↑	-	↑	-	-	↑	-	-	↓ Fiber diameter with use of oscillating air	
	Moore et al. (2004) [47]	↑↓	↑	-	-	↑	-	-	-	-	-	-	
	Marla & Shambaugh (2003) [48]	↓	-	-	-	-	↑	-	-	-	-	↑ Number of vibration modes	
	Marla & Shambaugh (2004) [49]	↓	↓	↑	-	-	-	-	↑	-	-	-	
Shambaugh, Papavassiliou & Shambaugh (2011) [50]	↓	-	-	-	↓	-	-	-	-	-	-	-	
Wadsworth	Straeffer & Goswami (1992) [51]	↑↓	↑	-	n/a*	-	↑	-	-	-	-	-	
	Jones & Wadsworth (1986) [52]	↑	-	-	-	-	-	-	-	-	↑	-	
	Choi et al. (1988) [53]	↓	-	-	-	-	-	↑	-	↑	-	-	
	Lee & Wadsworth (1990) [54]	↓	-	-	-	↑	-	-	↑	↑	n/a after 30 cm	-	
	Milligan et al. (1992) [55]	↓	-	↑	-	-	↑	-	-	-	-	↓ Fiber diameter with use of crossflow air	
	Sun et al. (1996) [56]	↓↑	↑	↑	-	-	-	↑	↑	-	-	-	
	Wente et al. (1954) [57]	↑↓	↑	-	-	-	-	↑	↑	↑	-	-	
	Zhang et al. (2002) [58]	↓↑	↑	↑	-	↑	-	-	↑	-	-	-	
	Yesil & Bhat (2016) [59]	↓	-	-	-	-	-	↑	↑	-	↑	-	
	Haynes (1991) [60]	↓	↓	-	-	-	↑	-	↑	↑	-	DCD is insignificant	
	Khan (1993) [61]	↓	↓	-	-	↑	-	-	-	-	-	DCD is insignificant	
	Malkan (1990) [62]	↑	↑	-	-	-	-	-	-	-	-	-	
	Feng et al. (2017) [63]	↓	-	-	-	-	-	-	-	-	↑	-	
	Guo et al. (2016) [64]	↓↑ No change	↑	-	-	-	-	-	↑	-	-	↑	-
	Ellison et al. (2007) [29]	↓↓	-	-	-	↑	-	-	-	-	-	-	↑ Air to polymer mass flux ratio
	Renukarn et al. (2016) [65]	↓↓	↓	-	-	-	-	-	-	-	-	-	↓ Spinneret diameter
	Tan et al. (2010) [13]	↑↑	-	-	-	-	-	-	-	-	-	-	↑ Melt viscosity ↑ Elasticity
	Hassan et al. (2013) [27]	↓	↓	-	-	-	-	-	-	-	-	-	-
	Jarecki et al. (2011) [66]	↓	-	-	-	-	-	-	↑	-	-	-	-
	Wang & Wang (2013) [67]	↓	-	-	-	-	↑	-	-	-	-	-	-
	Zeng et al. (2011) [68]	↓	-	-	-	-	↑	-	-	-	-	-	-
	Nayak et al. (2015) [69]	↓↓	-	-	↑	-	-	-	-	-	-	↑	-

Note. The * indicates a disagreement among researchers.

Table 5. Effect of MB process variables on basic nonwoven characteristics (adapted from [1] and upgraded based on the recent open literature)

Researchers	Independent Variables	Dependent Variables						
		Fiber Entanglement	Pore Structure (cover)	Mean Pore Size	Air Permeability	Tenacity	Elongation at Break	Other
Bresee & Qureshi (2004) [70]	↑ DCD	↓	↑	-	-	-	-	↓ Fiber orientation
Bresee et al. (2005) [71]	↑ Air flow rate	↓*	↓	-	-	-	-	↑ Fiber orientation
Uyttendaele & Shambaugh (1990) [45]	↑ DCD	-	-	-	-	-	-	↑ Fiber velocity ↓ Gas velocity
Wu & Shambaugh (1992) [72]	↑ DCD	-	-	-	-	-	-	↓ Fiber velocity (revised from 1990)
Straeffer & Goswami (1992) [51]	↑ Air flow rate	-	-	-	-	↑	↓	↑ Yield stress ↑ Initial modulus
	↓ Polymer flow rate	-	-	-	-	↑	↓	↑ Yield stress ↑ Initial modulus
Choi et al. (1988) [53]	↑ Die temperature	-	-	-	-	↓	↓	↓ Young's modulus ↓ Bending rigidity
	↑ Air pressure	-	-	-	-	↓	↓	↓ Young's modulus ↓ Bending rigidity
	↑ DCD	-	-	-	-	↓	↑	↓ Young's modulus ↓ Bending rigidity
Lee & Wadsworth (1990) [54]	↑ Processing temp. (die temp. & air temp.)	↑	-	↓	↓	-	-	-
	↑ Air flow rate	↑*	-	↓	↓	-	-	-
	↓ DCD	↑	-	↓	↓	-	-	-
Milligan et al. (1993) [55]	Use of crossflow air	↑	-	-	↑	↑	↑	↑ Bursting strength
Zhang et al. (2002) [58]	↑ Melt temperature	-	-	-	↓	↑	↓	↓ Hydrostatic head
	↑ Polymer flow rate	-	-	-	-	-	-	↓ Hydrostatic head ↓ Bulk density
	↑ Air temperature	-	-	-	-	↑	-	-
	↑ Air flow rate	-	-	-	-	↑	-	-
Uppal, Bhat, Eash & Akato (2012) [73]	↑ Air pressure	-	-	↓	-	-	-	↓ Number average fiber diameter ↑ Filtration efficiency
	↑ DCD	-	-	↓	-	-	-	↓ Number average fiber diameter ↑ Filtration efficiency
Khan (1993) [61]	↑ Air flow rate	-	-	-	↑	-	-	-
	↑ Polymer flow rate	-	-	-	-	↑	↓	-
Malkan (1990) [62]	↑ Polymer flow rate	-	-	-	↑	-	-	-
Qureshi (2001) [74]	↑ DCD	↑	-	-	-	-	-	↓ Fiber flow divergence
	↓ DCD	-	-	-	-	-	-	↑ Orientation in webs
Ghosal (2016) [75]	↑ Velocity of collector screen	-	↑	-	↑	-	-	-
Feng (2017) [63]	↑ DCD	-	↓	↓	-	-	-	↓ Stress ↓ Strain along length direction No change alignment degree No change apparent contact angle
Guo (2016) [64]	↑ Air temperature	-	No change	-	-	-	-	↑ Surface area
	↑ Polymer throughput	-	↓	-	-	-	-	↓ Surface area
	↑ DCD	-	↑	-	-	-	-	No change surface area
Bresee and Ko (2003) [9]	↑ DCD	↑	-	-	-	-	-	-
Zapletalova et al. (2006) [76]	↑ DCD	-	-	-	-	↓	↓	-

The MB technology is rather complex process, in which there are many different variables having impact on produced nonwovens such as polymer throughput, melt temperature, melt viscosity, air speed, air pressure, air temperature, die to collector distance (DCD), collector speed, die temperature and type of the die. Tables 4 and 5 show trends and conclusions that have been discovered for the last three decades. From the performed summarization, the following key conclusions can be deduced: 1) the average fiber diameter mainly depends on the throughput rate, melt viscosity, melt temperature, air temperature and air velocity. 2) For manufacturing the highest quality nonwovens is important to find a process window in which resulting nonwoven will have desired properties.

1.4 Flow instabilities and defects in melt blown technology

There is a number of flow instabilities and defects which can limit the processing window for the MB technology, especially with respect to smallest achievable fibers, namely:

- “Whipping” (fiber vibration)
- “Die drool”
- “Fiber breakup”
- “Melt spraying”
- “Flies”
- “Generation of small isolated spherical particles”
- “Shots”
- “Jam”
- “Nonuniform fiber diameters”

These flow instabilities are introduced below in more details.

Whipping – bending instability of thin liquid jets in air caused by large levels of melt/air inertia [11, 29, 68, 77 – 85]. Whipping in MB process is an aerodynamics driven bending instability [83]. The theory of aerodynamically driven bending instability of thin liquid jets in air was developed and described by Entov and Yarin [81, 84]. This bending instability is attributed to the high velocity of the air [68]. Higher air speeds lead to thinner jets and faster production rates, but also cause the fiber to undergo violent whipping motions. It is a possibility that whipping (and its associated defects) could be reduced by applying an air velocity field whose spreading character is minimized. Xie S. et al. discovered connection between the fluctuating characteristics of the velocity and temperature, which are caused by turbulent air flow field. Fluctuation of both velocity and temperature could account for the reason why the evenness of fiber diameter produced by MB was poor [85]. Therefore, annular (rather than 2D) air flows lead to a reduction in fiber distortions. Chung C. et al. found that melt inertia rather than melt rheology is the more dominant factor in controlling fiber shape [84].

Whipping can exist in two different cases:

- Two-dimensional bending motion, which is connected with slot-die (see Figure 6, left) where frequency and amplitude of fiber vibration can be changed in this trends:
 - frequency decreases as distance from the die head increases,
 - frequency decreases as polymer flow rate and temperature increase or if air flow rate decreases,
 - air temperature change does not have an effect on the frequency,
 - the amplitude increases as distance from the die head increases,
 - the amplitude increases when polymer flow rate decreases or if air flow rate increases,
 - the amplitude does not appear to change if either air temperature or polymer temperature are changed.
- Three-dimensional spiral path of fiber in post die area (see Figure 6, middle and right):
 - the frequency remains constant as distance from die head increases,
 - the amplitude remains constant for the given range of processing conditions,
 - the frequency decreases when polymer flow rate and temperature increases or if the air flow rate decreases,
 - the frequency is not air temperature dependent.

In general, higher amplitude and frequency of the fiber bending instability leads to the more uniform fiber laydown, which gives a better value for the end use of the MB nonwovens [80].

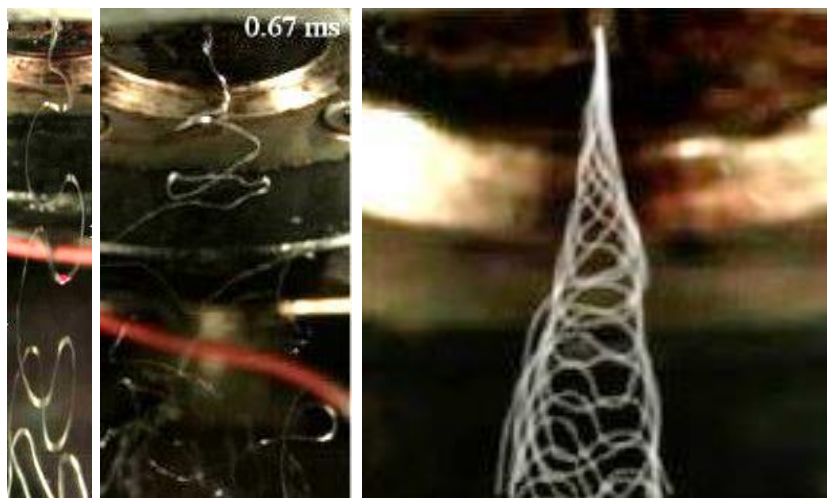


Fig. 6: 2D fiber bending instability (left) and 3D fiber spiral motion (middle, right) [77, 81]

Die drool – spontaneous accumulation of the polymer at the die exit (see Figure 7). Die drool can be eliminated via optimization of extrusion die design, polymer material or processing conditions [86].



Fig. 7: Die drool phenomenon occurring during extrusion of HDPE melt through a single hole [87] (left) and during melt blowing of PP via multi hole MB die under processing conditions provided in [Paper IV] (right)

Fiber breakup – instabilities that are driven by surface tension (for a Newtonian liquid the phenomenon is called Rayleigh instability) – surface tension forces cause fiber necking at different locations leading to pinch off the fiber (note that for viscoelastic melts, extensional stress build up due to drawing of the fiber can delay or even retard this instability [29] (see Figure 8). Ziabicki (1976) described, that fiber break up is caused by cohesive fracture and/or capillary action [11]. Ellison C. et al. observed that extent of fiber break up is dependent on both processing temperature and polymer and air flow rates [29]. Bresee R. suggested less fiber breakage to occur when primary air pressure is decreased and die to collector distance is increased [88]. Han W. et al. has found that polymer melt viscosity plays an important role in the fiber breakup and is affected by air temperature and pressure (i.e. that higher melt viscosity or lower air pressure could reduce the fiber breakup). It has also been observed that the polymer surface tension can increase dramatically with decreasing fiber diameter [89].

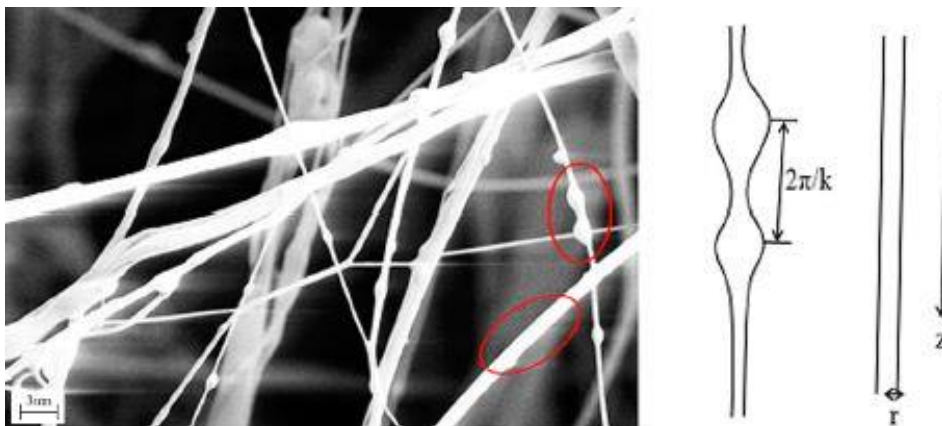


Fig. 8: Fiber breakup [89]

Melt spraying – significant fiber breakup [29, 81, 84, 90], see Figure 9.



Fig. 9: Melt spraying [78]

Flies – creation of very short fine fibers, which contaminate the surroundings, because they do not collect on the collector (see Figure 10). This phenomenon is caused by the extreme and excessive blowing conditions that cause fiber breakage (air pressure, die to collector distance, collector speed) [27, 29, 88, 91]. Hassan M. et al. [27], Tan D. et al. [93] and Moore E. et al. [47] have found that very high air velocities (supersonic flow) produce unstable air flow field which is responsible for a large quantity unbound fibers (flies). Individual fly particles can contain as much as 150 m of fiber length [88]. Fly formation is controlled primarily by aerodynamic drag and fiber entanglement. Fly particles are released when a drag force is strong enough to break fibers and fiber entanglement is insufficient to retain broken fibers within the forming web [88]. Bresee R. and Qureshi U. showed that only two regions of the basic MB process are likely to produce a large drag force on fiber. These regions are located near the die and near the collector where differences between air and fiber speeds are large [88].

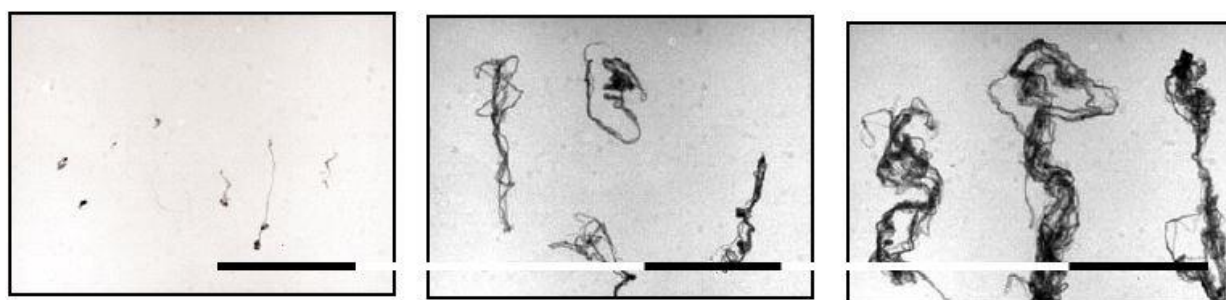


*Fig. 10: Flies collected at high (left), medium (middle) and low (right) DCD [88].
The length of the black bar is 3.0 cm*

Generation of small isolated spherical particles – it is assumed that the origin of the spheres is a result of fiber breakup instabilities [29]. Such small spherical particles are intermingled amongst the fibers (see Figure 11) and some of them are able to escape from the produced mats during their collection.

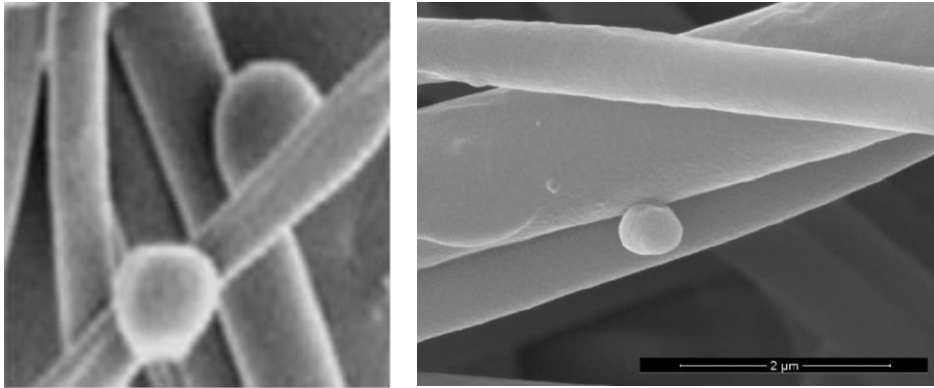


Fig. 11: Visualization of isolated spherical particles on the produced mat [29, 93]

Shots – creation of small (usually degraded) round clumps of polymer in the web that have ill-defined shape (see Figure 12). It can be caused by excessively high temperature, too low polymer molecular weight, or poor equipment cleanliness. Shots are generally attributed to the breakage of the fibers as they are being drawn in the air stream [3, 4, 17, 29, 94, 95].

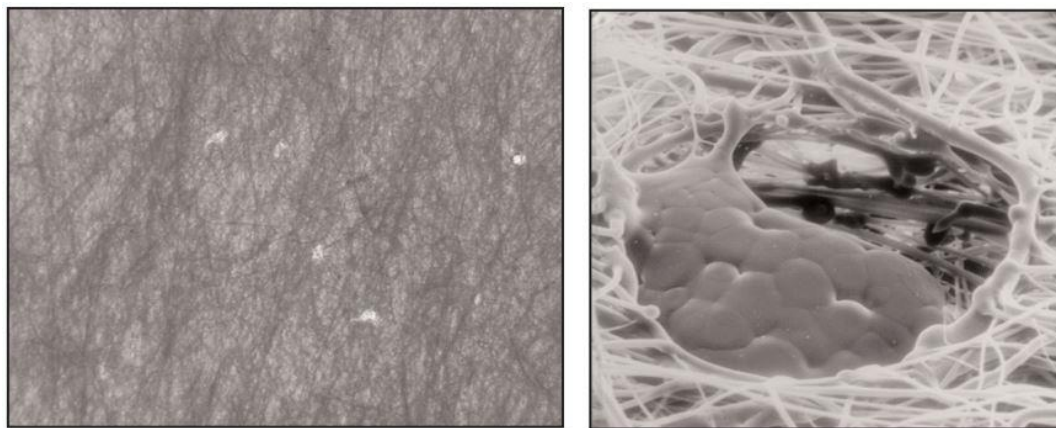


Fig. 12: Damaged web due to shots (left) including detail view for one shot (right) [95]

Jam – fibers accumulation in space due to adhesion between fiber segments (see Figure 13) occurring during fiber speed decrease through the majority of the die to collector distance, which contributes to fiber disorientation and creation of entanglements between the fibers [84].

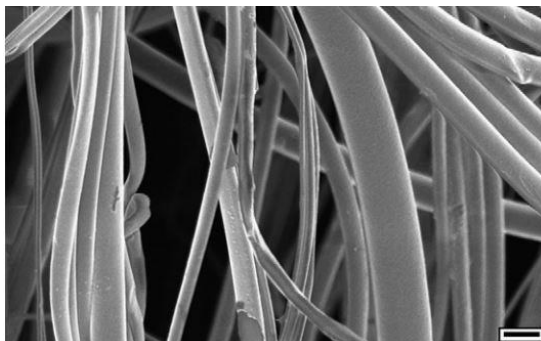


Fig. 13: Jam effect [29]

Nonuniform fiber diameters – it has been discovered that fiber diameter distribution for MB nonwovens can be well described by a log-normal distribution function regardless of average fiber diameter [13] (see Figure 14). Bates et al. found the trends between melt viscosity and elasticity vs. average fiber diameter and coefficient of variation (CV). In more detail, they observed that increase in melt viscosity leads to an increase in average fiber diameter with almost no effect on CV. On the other hand, it has been revealed that increase in the melt elasticity appears to decrease CV and increase average fiber diameter [13, 29, 31, 32, 96].

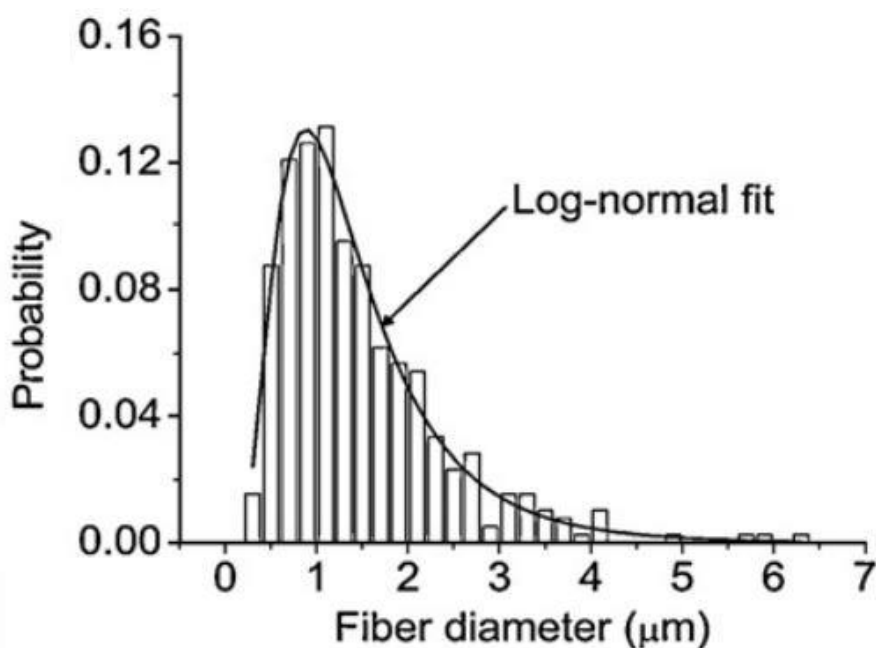


Fig. 14: Typical fiber diameter log-normal distribution for MB nonwoven [13]

2. POLYPROPYLENE

2.1 Linear polypropylene

As it was mentioned before, the PP is the most used polymeric material in the production of nonwovens by MB technology. To stabilize the manufacturing process, it is necessary to know the behavior of polymers under the conditions that prevail in the MB process. It is both thermal stability as well as rheological behavior a high shear strain rates. PP occurs in two basic types (**linear** Figure 15, left and **branched** Figure 15, right) and is usually processed in a melt state.



Fig. 15: Linear (left) and branched structure (right) of PP

A clear understanding and control of the structural changes is absolutely essential. During processing of PPs, degradation reactions can start to occur, which can significantly influence their molecular structure, narrow the processing window, as well as reduce basic properties of the final product considerably. The most attention has been focused on conventional linear PPs. In more detail, it has been shown that free-radical-induced degradation of PP, induced by different amounts of peroxide, leads to reduction in average molecular weight, polydispersity and melt viscosity [97 – 103]. Thermo-mechanical and/or thermo-oxidative degradation of PPs was investigated by using the multiple extrusion process [104 – 106], torque rheometer [107], rheometric mechanical spectrometer [108], and windy oven [109]. It has been demonstrated that Newtonian viscosity [105], recoverable shear compliance [105], molecular weight [104], loss and storage moduli [108] monotonically decrease with the degradation time mainly due to chain scission of macromolecules driven via β -scission reaction, breakdown of peroxy radicals and shear [104]. It has been found that during thermo-mechanical degradation, the chain scission at low molecular weight (MW) is random (i.e., MW-independent) but it is increasing with MW at higher MW, which is in good agreement with mechanical degradation theory of Bueche, which states that “the probability of

chain scission is higher for the high MW chains to yield smaller molecules of about half the original size” [106]. The situation was found to be even more complex during thermo-oxidative degradation, during which chain scission can be kinetically favored near the oxygen-centred radicals leading to a heterogeneous type of degradation and causing change from unimodal to bimodal molecular weight distribution [109]. Even if the degradation behavior of conventional linear PP is well documented in the open literature, only a little or no information is known about structural changes during thermal degradation of branched PPs, especially with respect to branching, which could be used for process stabilization and optimization of final product properties.

2.2 Branched polypropylene

The key problem with processing of conventional linear PP is its low melt strength, which may limit processing window considerably. The melt strength properties of a polymer increases with molecular weight and with long-chain branching due to the increase in the entanglement level. That is reason why the considerable progress has been made to enhance PP melt strength by introducing of long chain branching (LCB) via different methods such as:

- **Electron beam radiation** [110 – 116] – influence the molecular structure of polymer. Results of the researches indicate that there is a competition between degradation and branching. The amount of irradiation dose, irradiation atmosphere and monomer concentration are factors that influence the competition between chain scission and branching reaction. Mousavi et al. [111] discovered the increasing dominance of branching under air atmosphere. Krause at al. [113] found a relationship between an irradiation temperature and level of branches. At higher temperature (200 °C vs. 25 °C), generation of highly higher branched structure is more probable. Auhl et al. [114] have found that at higher doses a star-like architecture is changed to a tree-like branching architecture with shorter molecular segments.
- **Gamma radiation** [110, 116 – 118] – the molecular structure of irradiated polymers is a result of branching, crosslinking, and degradation by chain scission reactions. The polymers irradiated by gamma radiation exhibit a branching structure which is similar to a slightly branched LDPE, while

electron beam irradiation led to branched molecules, which carry fewer but probably longer long chain branches.

- **UV radiation** [119 – 126] – the final PP molecular structure is affected by photoinitiator concentration, radiation time, UV lamp intensity, radiation temperature and type of photoinitiator used. Different combinations of these variables can result in controlled PP rheology, long chain branched PP or even crosslinked PP, if the radiation time is long enough.
- **Utilizing peroxides** (usually in presence of multifunctional monomers) [127 – 133] – long chain branches could be added to initially linear PP using reactive extrusion in the presence of selected organic peroxydicarbonates (PODIC). The modification of PP with specific peroxydicarbonates leads to long chain branching and improved melt strength. The amount of long chain branches can be controlled by the type and the amount of PODIC used for the modification. The shear viscosity at high shear rates is not much affected by the modifications. The zero-shear viscosity, however, increase considerably with the addition of a few branches, and the increase may be related to the degree of branching.

As it was mentioned above, long chain branching has a profound effect on the process ability of polymeric materials. For polyolefin processing is crucial to understand the effect of the type and amount of LCB. It has been shown that rheological measurements are very sensitive to even small amounts of LCB. That is reason why the combination of typical methods to characterization of branching degree (size exclusion chromatography, nuclear magnetic resonance) and the rheology is really effective for describe completely polymeric structure. Interesting tool for deduce the branching structure of polymers is the dependence of zero shear rate viscosity on the weight average molecular weight. Zero shear viscosity for the branched PP is higher than the linear PP, which might imply a slightly branched polymer with a star-like branching structure. In case of PE, the trend is opposite. The branched PE has lower zero shear viscosity when compared with the similar average molecular weight of linear PE. This means that a branched PE is highly branched with a tree-like branching structure [134].

Branched PP is thermorheologically simple whereas branched PE is thermorheologically complex. Thermorheologically simple response means that the frequency dependent $G'(\omega)$ and $G''(\omega)$ values superimpose at different

temperatures, while the thermorheologically complex materials exhibit a systematic split between the curves with temperature. For both the PP and PE blends, the degree of elasticity was found to be decreasing with the weight fraction of the long chain branched polymer [134]. Analysis of the temperature dependencies of the basic rheological properties was also found to be a useful tool to understand the branching structure of polymers [134].

Another significant indicator of branching topology and molecular structure is the flow activation energy. It has been revealed that branched polymers exhibit higher flow activation energies than linear ones of similar weight average molecular weights. The value of the flow activation energy for linear PP is located typically in the range 36 – 44 kJ/mol, but for long chain branched PP a value about of 70 – 80 kJ/mol was found [134, 135]. The flow activation energy dependence on the fraction of branched polymer has been found to be different for PP and PE blends which might be because of difference in the type of branching. However, generally, the flow activation increases with the increasing of long chain branching fraction [134]. Molecular structure of polymer samples is important for the occurrence of extensional strain hardening phenomenon. In terms of chain topology, strain hardening is caused by LCB. Just note that strain hardening means the rise of the elongational viscosity above the zero rate elongational viscosity [134 – 136].

It can be said that branched PPs have a predominantly star-like structure [114, 116, 134, 137 – 139], which causes significant extensional strain hardening inducing a so-called “self-healing” effect leading to improved quality of products (for example, wall thickness uniformity or a better foam structure) due to homogeneous deformation in elongational flows [139 – 143], a more pronounced shear thinning behavior, and a higher elasticity compared to linear PP [129, 133, 144, 145].

3. HIGH SHEAR RHEOLOGY

In the MB process, the specially developed polymeric materials with extremely high MFI (typically 300 – 2,000 g/10min) are used and processed at large deformation speeds ($\sim 10^6 \text{ s}^{-1}$), as has been mentioned in the previous chapters. However, very little information is known about the rheological behavior of polymer melts in these high shear rates. To optimize the industrial processes and tailor the material properties, a thorough knowledge of the flow behavior across a wide range of deformation rates and temperatures is necessary. These data cannot be measured using conventional rheometers only. Attainable shear rates in rotational rheometry are limited from 10^{-4} to 10^1 s^{-1} and for capillary rheometry from 10^1 to 10^5 s^{-1} . In the past decade, only few studies were focused on the rheological evaluation of these very low viscosity materials for low and medium deformation rates (from 0.5 to 80,000 s^{-1}) [7, 38, 146, 147]. The rheological investigation of low viscosity polymeric materials, such as MB PPs, at very high shear deformation rate range ($10^5 - 10^7 \text{ s}^{-1}$) has not been performed yet. However, it should be mentioned that some publications have already been spotlighted on rheology of common polymer melts behavior (HDPE, LDPE, PP, PS, polymethylmethacrylate (PMMA), ultra high molecular polyethylene (UHMWPE), styrene acrylonitrile (SAN)) at high shear rates [148 – 155]. Due to the impossibility to use conventional measuring methods, new or modified existing rheometers have been used. Mnekbi et al. [153] used basic capillary rheometer with six different dies, diameter D equal to 1 mm and 0.5 mm, and length over diameter L/D ratio equal to 4, 8 and 16. High shear rates values up to 10^5 s^{-1} have been reached in this case. Takahashi et al. [154] designed special capillary rheometer, which consists of a die (nozzle) and a specially designed injection unit. Dies with various sizes of capillaries 0.4 – 1 mm and length 2.5 – 20 mm were used. The capillary of 0.5 mm diameter and 10 mm length was the most used and the shear rate above 10^6 s^{-1} were reached. Rides et al. [148], Chen et al. [149] and Kelly et al. [151] took advantage of instrumented nozzle adaptor fitted with a die of 4 mm length and 0.5 mm diameter or 10 mm length and 0.3 mm diameter, which is connector to injection molding machine. In their research, rheological measurements were possible in the shear rate range up to 10^7 s^{-1} . Friesenbichler et al. [152] suggested a special injection mold with interchangeable conical slit-die inserts with varying slit heights. In order to achieve a wide range of practically relevant shear rates, three dies with different slit heights 1 mm, 0.5 mm and 0.35 mm, entrance angle of 60° were used. In this work, shear rates up to 10^5 s^{-1} were achieved. It should be noted that shear

heating and pressure dependence effects usually take the place during the polymer melt flow at high shear rate range, which may potentially limit determination of reliable viscosity data.

In more detail, Guan et al. [155] and Chen et al. [149] discovered that three effects (end pressure loss, dissipative heating and pressure dependence) have a significant effect on the shear viscosity for different polymers obtained via capillary rheometry. They have found that the end effect for the PS melt flow increases the most rapidly with shear rate and becomes pronounced at shear rates above $2 \times 10^5 \text{ s}^{-1}$ whereas for PP and LLDPE it was $8 \times 10^5 \text{ s}^{-1}$ and $2.8 \times 10^6 \text{ s}^{-1}$, respectively. The significance of the end effect was ordered as PS>PP>LLDPE. It was speculated that for given polymers and processing conditions, the end effect was dominant over the other two effects. Further, the dissipation effect was found to be less significant at lower shear rates (up to about 10^5 s^{-1}) than pressure effect but the situation was switched at higher shear rates (i.e. roughly between $10^5 - 10^6 \text{ s}^{-1}$).

Kelly et al. [151] and Rides et al. [148] observed uncommon behavior for LDPE, PS and PMMA melts. Measured shear viscosity exhibited a deviation from pseudoplastic shear thinning behavior at high strain rates, initially following a second Newtonian type plateau and then demonstrating shear thickening behavior. This behavior was attributed to particular molecular structure of investigated polymers and their compressibility. They found that polymers with larger side groups such as PS reaching a second Newtonian plateau at lower shear rates in comparison with PP and PE samples.

Takahashi et al. [154] investigated rheological behavior of HDPE, UHMWPE, PP, PS and SAN at shear rates up to 10^7 s^{-1} . Two non-Newtonian regions and a transition or second Newtonian region were observed. The behavior of investigated polymers melts was categorized into three possible flow regimes, see Figure 16. The first regime is characterized by a development of clear second Newtonian region occurring after the first non-Newtonian region. This behavior was measured for HDPE, UHMWPE and PP. In second flow regime, the transition region appears instead of a second Newtonian region. This feature was observed for PS. The third flow regime is described as an intermediate step between the previous categories. The third flow regime was observed for SAN

and PA-6,6. From the measured rheological data, the authors formulated the following conclusions: in the first non-Newtonian region, viscosity depends on the entanglement density and in the second non-Newtonian region; the viscosity depends mainly on polymer scission. It was concluded that, in the second Newtonian or transition region, the viscosity depends only on the friction of highly oriented molecules in which all the entanglements vanish and molecular scission occurs beyond a critical shear rate.

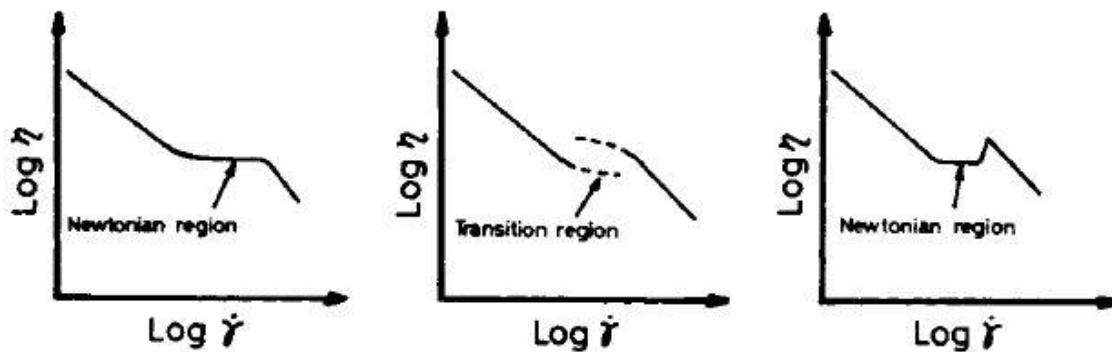


Fig. 16: Three flow regimes observed in flow curves for different polymer melts [154]

Mnekbi et al. [153] investigated the rheology of a HDPE at high shear rates. The rheological data was fitted by Carreau-Yasuda model. It was deduced that at high shear rates, the heat dissipation and pressure effect decreases and increases the total pressure drop, respectively. It was concluded that these two effects are cancelled out mutually at shear rate until 10^5 s^{-1} .

THE AIMS OF THE DOCTORAL RESEARCH WORK

The main aim of the doctoral research work is to investigate the complicated relationship between polymer melt rheology, molecular structure of polymers, process conditions and formation of polymeric nanofibers produced via melt blown technology. For such purpose, different polypropylenes (namely linear, branched and their blends) having well defined molecular architecture will be chosen and rheologically characterized utilizing different constitutive equations. Then, the chosen polypropylenes will be used to produce polymeric nanofibers on the melt blown pilot plant. In more detail, the key presented Ph.D. thesis aims can be defined as follows:

- Evaluation of thermally induced molecular changes of branched polypropylene via rheology and different constitutive equations.
- Measurements and modeling of low and high flow rate rheology of melt blown polypropylenes having different molecular weight, molecular weight distribution and varying level/amount of chain branching.
- Instrumented injection molding machine will be utilized to measure the rheology at strain rates above those attained during conventional rheometry. If necessary, novel constitutive equation will be developed to describe experimental reality.
- Based on the performed rheological study and modeling, carefully selected polyolefins/polyolefine mixtures will be used to produce nanofiber nonwovens on the melt blown pilot plant line having 250 mm active die width. It is considered that the following parameters will be systematically varied: melt temperature, die to collector distance, collector belt speed, air speed and mass flow rate. The most challenging point to fulfill this aim is to properly determine basic morphological characteristics of the nanofiber based melt blown nonwovens in order to perform particular correlations.

4. MATERIALS AND INSTRUMENTS

In the presented Ph.D. thesis, different PP homopolymers (linear and branched), their blends as well as variety of instruments are utilized. Basic characteristics of chosen polymers are summarized in Table 6, whereas description of particular instruments is provided in Chapter 4.1.

Table 6. Basic characteristics for chosen PPs (pellets)

	M_n^* (g mol ⁻¹)	M_w^{**} (g mol ⁻¹)	M_z^{***} (g mol ⁻¹)	M_{z+1}^{****} (g mol ⁻¹)	$M_w/M_n^{\#}$ (-)	Melt flow index (2.16 kg/230 °C) (g/10min)	DSC peak melting point (°C)
LCB-PP Daploy WB180HMS	37,200	266,500	877,500	1715,000	7.16	6	154
L-PP HL504FB	20,100	112,500	284,500	510,500	5.60	450	161-165
L-PP HL508FB	17,050	104,500	282,000	533,000	6.13	800	156-160
L-PP HL512FB	16,950	90,950	220,500	384,500	5.37	1200	156-160
L-PP/LCB-PP BLEND 1	17,700	102,000	286,000	603,000	5.76	800	-
L-PP/LCB-PP BLEND 2	18,650	112,500	342,000	775,500	6.03	615	-
L-PP/LCB-PP BLEND 3	20,050	126,000	403,000	896,500	6.28	440	-

- * M_n – Weight-average molecular weight
- ** M_w – Number-average molecular weight
- *** M_z – Z-average molecular weight
- **** M_{z+1} – Z+1-average molecular weight
- # M_w/M_n – Polydispersity index

4.1 Rotational Rheometer (ARES 2000)

Rotational rheometer *Advanced Rheometric Expansion System* (ARES 2000, Rheometrics Scientific, USA) equipped with 2K FRTN1 and 2K FRTN2 transducers (see Figure 17) has been used for measurements in both oscillatory and steady state modes. Rotational rheometer has been used in parallel plates configuration (25 mm plates diameter). For extremely low viscosity polymers, a special aluminum plate with the overflow channel was used (see Figure 18). Linear viscoelastic properties (storage modulus G' , loss modulus G'' , and complex viscosity η^*) have been measured in oscillatory mode as well as thermal stability test, whereas Newtonian shear viscosity of branched high molecular weight PPs was measured via creep test for low enough shear stress (70 – 550 Pa). The Newtonian viscosity of very low molecular weight PPs was

measured in an oscillatory mode, in which frequencies were varied from 0.1 up to 100 $\text{rad}\cdot\text{s}^{-1}$ and shear strain was chosen 1 % to guarantee linear viscoelastic regime. In order to capture the largest possible range of the shear rates, the measurement was performed at temperature step of 10 °C from 170 °C up to 230 °C. Then, time temperature superposition principle was used to create mastercurve at one reference temperature 180 °C. The thermal stability measurements have also been carried out at 180 °C under inert N_2 gas atmosphere for all samples to prevent their oxidative degradation.



Fig. 17: Rotational rheometer ARES 2000

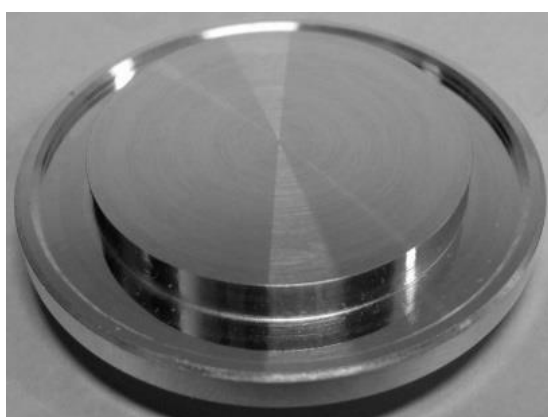


Fig. 18: Aluminum plate with the overflow channel

4.2 Extensional Rheometer (SER-HV-A01)

Transient uniaxial extensional viscosity has been measured by Sentmanat Extensional Rheometer (SER-HV-A01 model, Xpansion Instruments, USA) attached to ARES 2000. This novel detachable fixture includes dual wind-up drums rotating in opposite directions to guarantee uniaxial extensional deformation (see Figure 19). Compression molding was used to produce thin plates, a dual blade cutter for preparation of samples with fixed 12.7 mm width and a micrometer to determine sample thickness. With the aid of SER instrument, the branched high molecular weight PPs were tested at 12 applied extensional rates (10, 5, 3.16, 1, 0.5, 0.316, 0.1, 0.05, 0.0316, 0.01, 0.005, 0.00316 s^{-1}) and at three different temperatures (170 °C, 180 °C and 190 °C). The obtained data were shifted to the reference temperature 180 °C. The ‘steady state’ uniaxial extensional viscosity data were taken from the peaks appearing on the transient extensional viscosity curves for corresponding extensional strain rate.

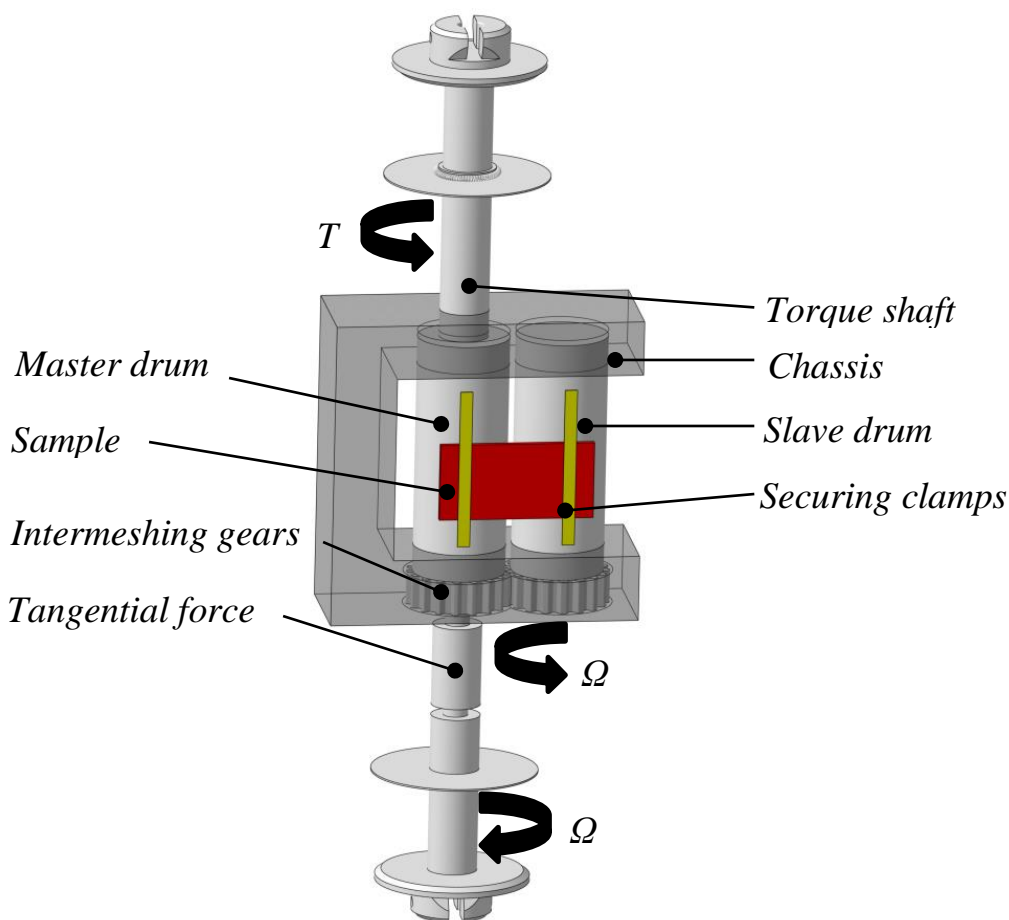


Fig. 19: Sentmanat Extensional Rheometer (SER-HV-A01)[156]

4.3 Capillary Rheometer (Rosand RH7-2)

The twin bore capillary rheometer Rosand RH7-2 (Rosand Precision, Ltd., Great Britain) has been used for measurement steady state shear viscosity (annular capillary die configuration), uniaxial elongational viscosity at high shear rates and controlled thermal degradation of chosen PPs. A schematic 3D section view of this device is displayed in Figure 20.

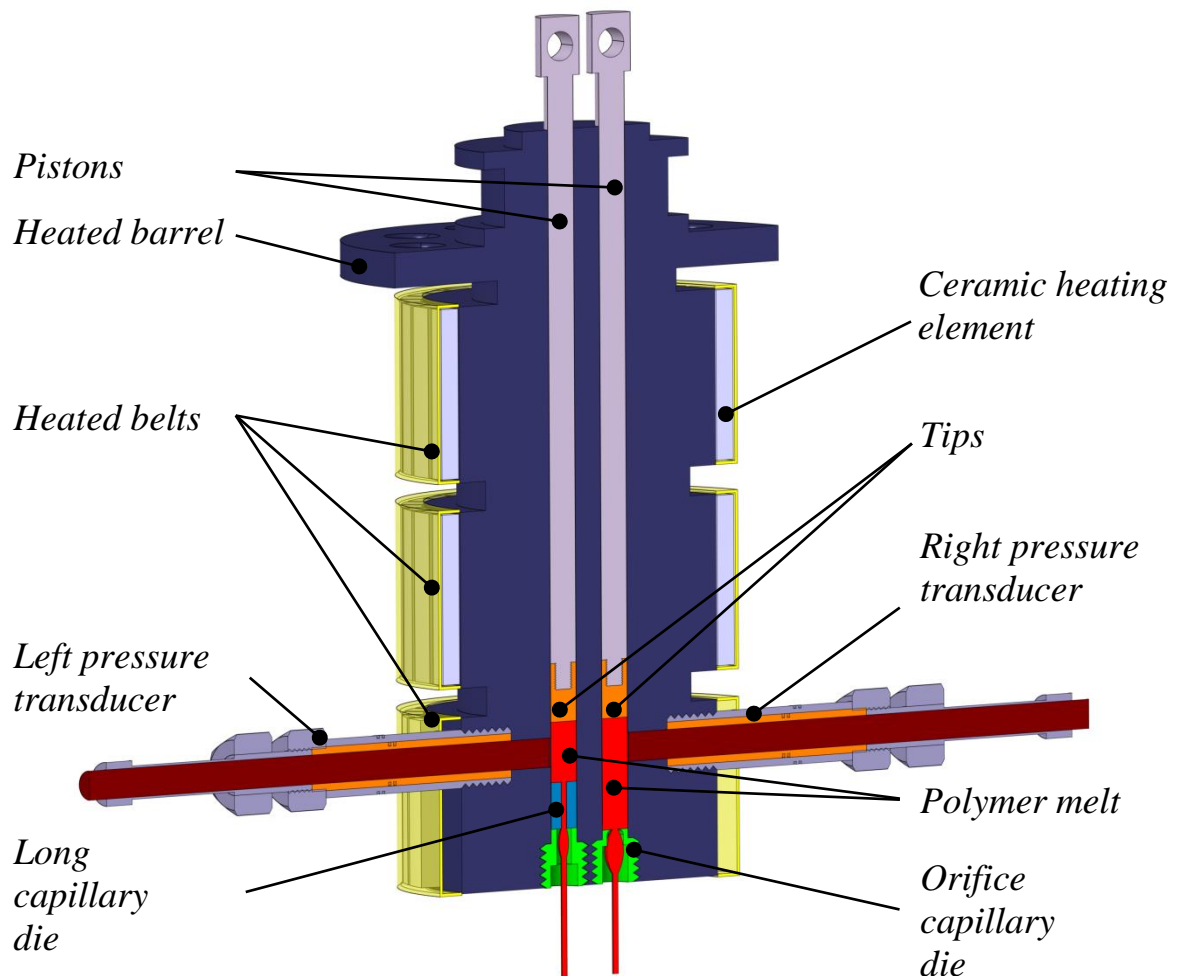


Fig. 20: Cross-section of twin-bore capillary rheometer

Capillary rheometer operates on the principle of pushing the polymer melt in the controlled way through a defined capillary die with simultaneous recording of corresponding pressure drops. Two measurements are usually performed simultaneously at the same time on two capillary dies having the same diameter but different length (long die and the orifice die with zero length). All capillaries, which have been utilized in this work, have open downstream region, which does not allow any polymer melt sticking at the die exit wall. Therefore, the measured entrance pressure drop can be considered to be very precise. A constant piston

speed mode was used in all experiments (max. piston speed 600 mm/min) at 190 °C, 210 °C, 230 °C and shear rates 30 – 640,000 s⁻¹. Two preheating steps (taking 3 and 6 minutes) were applied before each measurement with the aim to compact the polymer granules and remove air bubbles. In order to determine the pressure drop through given dies at very wide range of deformation rates for all polymer samples, different pressure transducers (Dynisco, USA) in ranges of 10,000 PSI (68.9476 MPa); 1,500 PSI (10.3421 MPa); 500 PSI (3.4473 MPa) and 250 PSI (1.7237 MPa) were utilized. For shear and uniaxial extensional viscosities determination, capillaries with diameter of 3 mm, 1 mm, 0.5 mm, 0.15 mm and L/D equal to 0 (orifice die), 14 and 16 (long die) were used.

4.4 Fanuc Roboshot S-2000i 100A

High strain rate rheometry has been measured by Fanuc Roboshot S-2000i 100A injection molding machine (see Figure 21) with screw diameter 22 mm and a maximum barrel pressure rating of 240 MPa. The machine was operated in air-shot mode using an instrumented rheometric capillary die nozzle (see Figure 22). The section of the used assembly is depicted in Figure 23, whereas each individual part is displayed in Figure 24. Melt pressure was measured at the capillary die entrance at a frequency of 100 Hz using a Kistler 4021A pressure transducer (range 0 – 300 MPa). Injection screw position and velocity were also monitored at the same frequency. Polymer was injected over a velocity range of 2.6 mm/s to 220 mm/s firstly through a capillary die of 8 mm length and diameter 0.5 mm, and then tests were repeated with an orifice die of the same diameter enabling Bagley and Rabinowitsch corrections. Polymer was plasticized in the screw of the molding machine at a screw rotation speed of 2.83 revolutions per second with a back pressure of 0.1 MPa. Injection was initiated following a dwell time of 30 s. Process data were collected using a LabView SC2345 data acquisition unit triggered by a 24 V signal from the injection molding machine at the start of injection. All rheological measurements were carried out at three different temperatures (190 °C, 210 °C and 230 °C) for given polymer samples.



Fig. 21: Fanuc Roboshot S-2000i 100A [157]

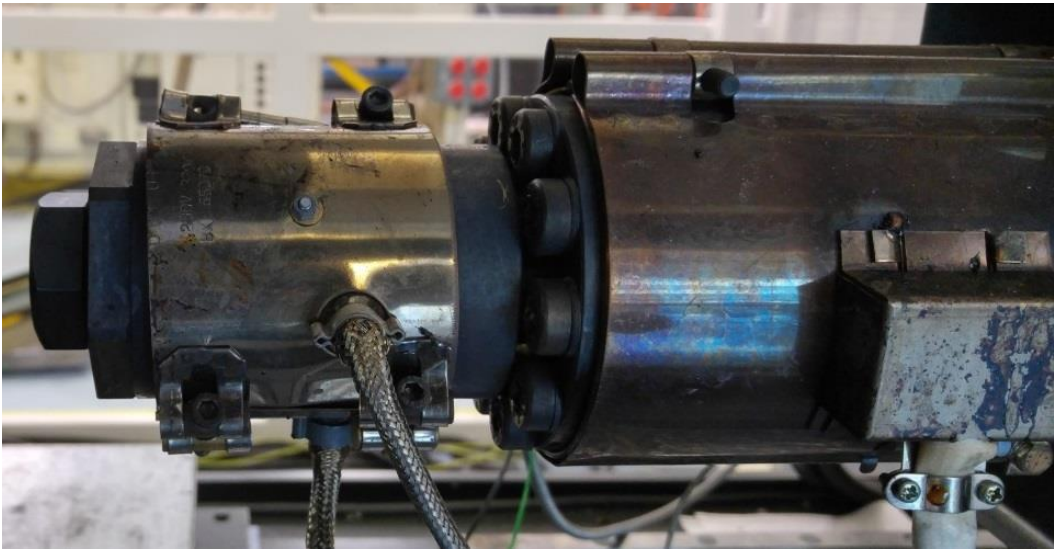


Fig. 22: Detail view of nozzle adapter connected to injection unit

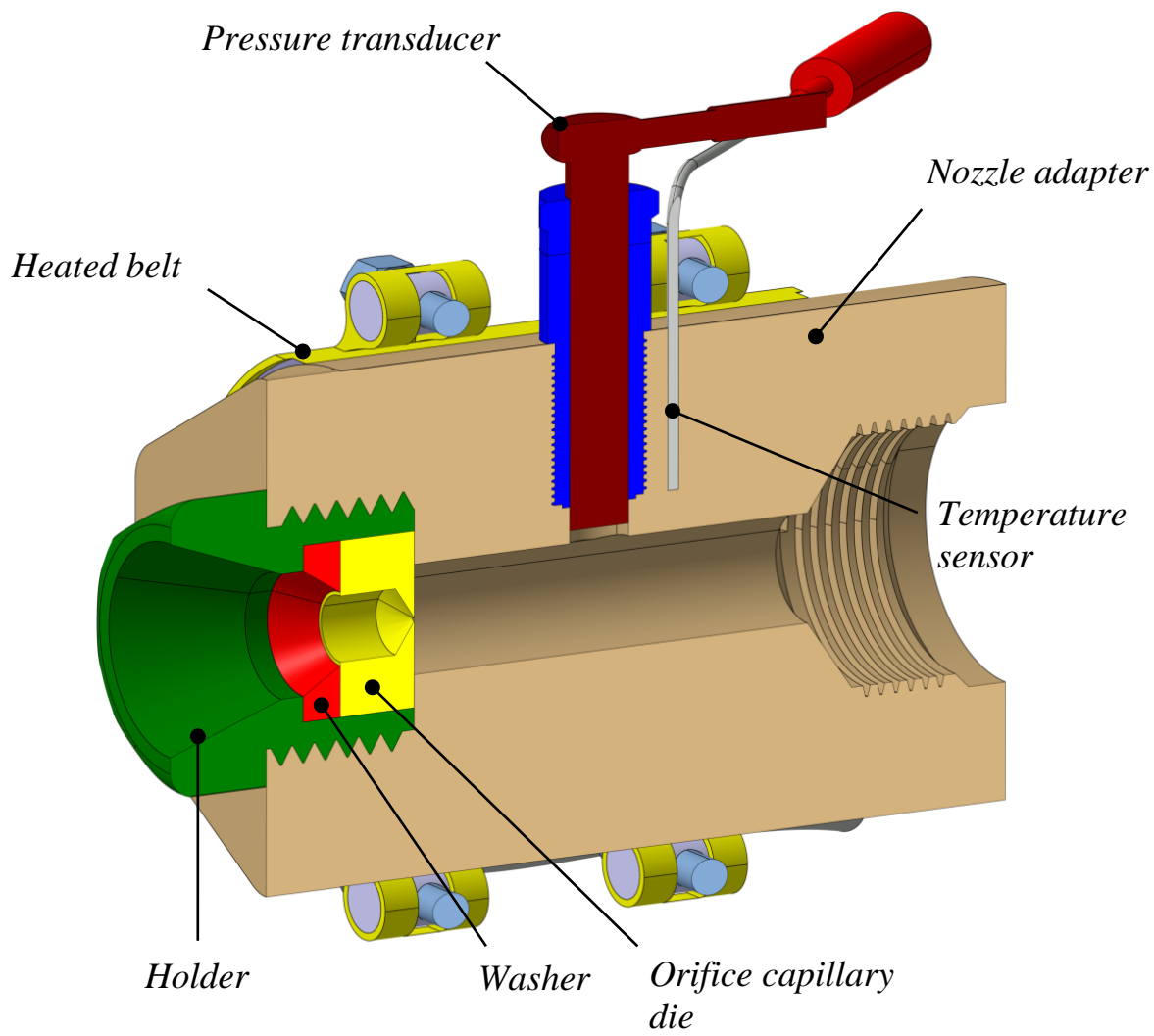


Fig. 23: Cross-section of assembled parts for the instruments injection molding machine

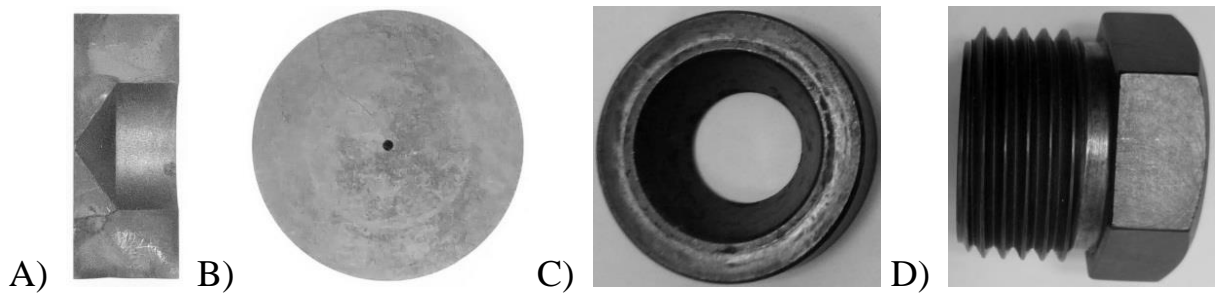


Fig. 24: Photo of A) orifice capillary die B) long die C) washer and D) holder utilized during high shear rate measurements

Next step was production of nonwovens from all polymer melts on pilot MB line with the aim to analyze their performance in relation to processing conditions and chosen polymer melt.

4.5 Reifenhäuser REICOFIL pilot melt blown line

Nonwoven samples from chosen polymer samples were produced on the Reifenhäuser REICOFIL pilot plant MB line, which is depicted in Figure 25. The diagram of MB line was described in previous section 1.2. It should be mentioned that the die nosepiece (sharp die) visualized in Figure 26 has following characteristics: total and active width equal to 350 mm and 250 mm, respectively; orifice diameter: 0.4 mm; number of holes per active part: 470; processing conditions: melt/air temperature 270 °C; collector belt speed: 4 m/min, die to collector distances: 200 and 500 mm. Air volume flow rate was adjusted to be about 390 m³/hr for given processing conditions and used polymer to reach the same average fiber diameter for all samples, i.e. 1604±86 nm, keeping the mass flow rate for one orifice the same (0.088493 g/min).



Fig. 25: MB pilot line for two different processing conditions: (left) DCD = 500 cm, (right) DCD = 200 cm

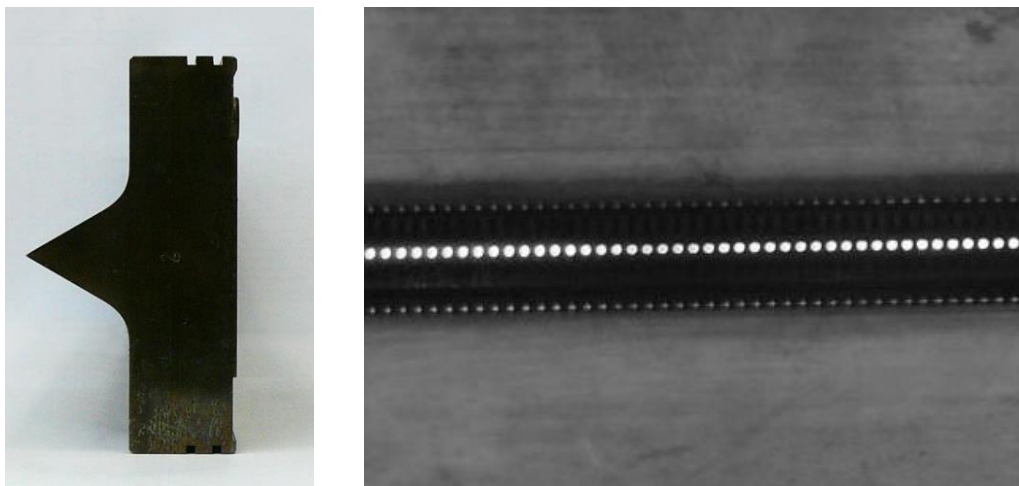


Fig. 26: Detailed view of utilized MB die (left – side view, right – front view showing 0.4 mm diameter holes)

4.6 HITACHI Tabletop TM-1000 SEM microscope

In order to determine basic morphological characteristics of produced MB nonwoven webs, Tabletop TM-1000 scanning electron microscope (SEM) was used. Before taking an image, a sample from the produced nonwoven was cut out and coated in sputtering device. In this work, Polaron SC7640 sputtering device visualized in Figure 27 has been used for sample coating under the following conditions: argon as inert atmosphere, palladium as coating material, plasma current 25 mA, voltage 2.1 kV, chamber pressure 6 Pa and all this for 60 seconds. After preparing of all samples in sputtering device, SEM pictures were taken by HITACHI Tabletop TM-1000 which is depicted in Figure 28. Tabletop TM-1000 operates with an accelerating voltage 15 kV, electron gun: pre-centered cartridge filament, vacuum pump: turbomolecular pump 30 l/s \times 1 unit and detection system: high-sensitive semiconductor BSE detector. The images were taken in various sets, magnifications (500 \times , 1,000 \times and 2,500 \times) and focus areas. Captured images are in BMP format with resolution 1,280 \times 960 pixels.



Fig. 27: Polaron SC7640 sputtering device [158]



Fig. 28: Visualization of HITACHI Tabletop TM-1000 SEM microscope

SUMMARIZATION OF THE SELECTED RESEARCH RESULTS

Rheological characterization of long chain branched polypropylene Daploy WB180HMS (LCB-PP) [Paper I]

It was shown that the studied branched high molecular weight PP Daploy WB180HMS is thermorheologically simple showing simultaneous occurrence of chain scission and branching during thermal degradation. In more detail, complex viscosity, shear elasticity, Newtonian viscosity and average relaxation time was found to decrease with the degradation time within first 3 h, then increase up to the local maximum at five hours and finally decrease again indicating simultaneous occurrence of the chain scission and recombination reactions (see example for the Newtonian viscosity in Figure 29).

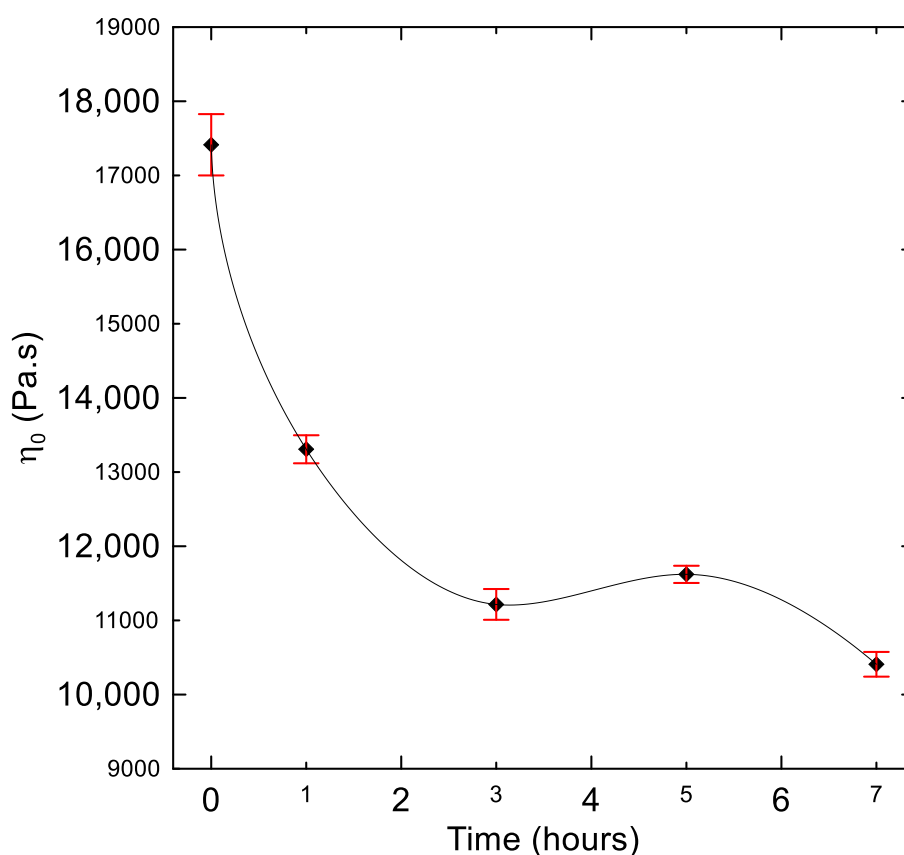


Fig. 29: Newtonian viscosity, η_0 , for virgin and degraded PPs obtained from shear creep measurements at 180 °C

This rheological observation was found to be in good correspondence with the changes in polydispersity index M_w/M_n , M_z and M_{z+1} molecular weight averages. Consequent analysis of the virgin and thermally degraded polymer melts in the uniaxial extensional flows has revealed that the level of extensional strain hardening (i.e., the level of chain branching) increases within the first three hours of thermal degradation and then decreases (see Figure 30). This indicated dominance of recombination and scission reactions on the chain branches before and after 3 h of thermal degradation, respectively.

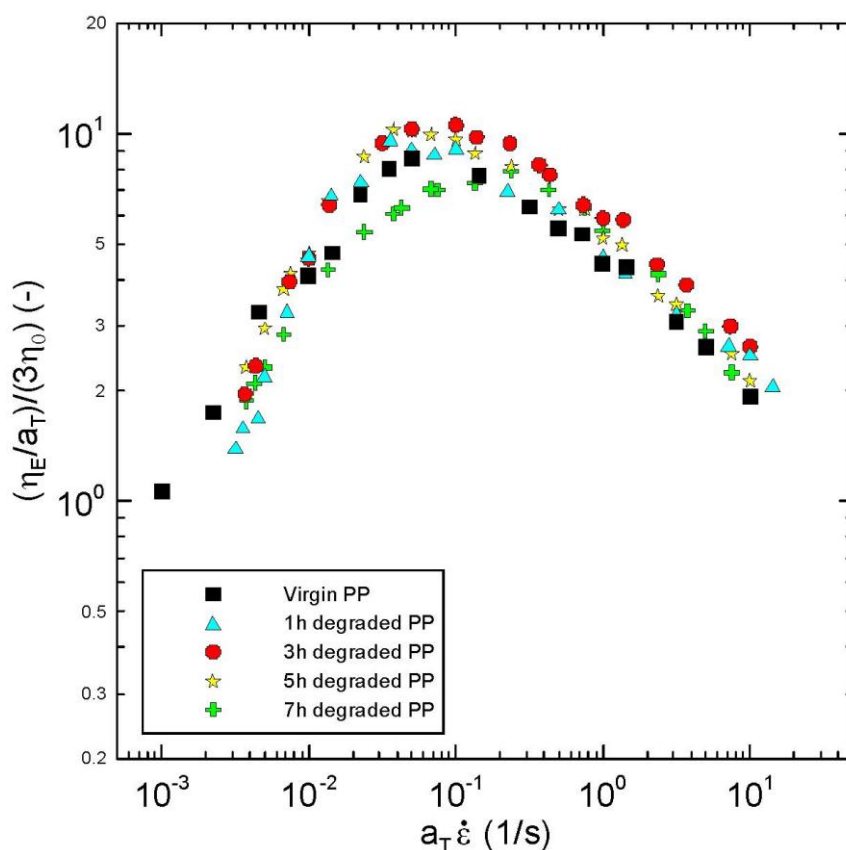


Fig. 30: Reduced steady-state uniaxial extensional viscosity, η_E/a_T , data at 180 °C normalized by the three-fold Newtonian viscosity, $3\eta_0$, for virgin and thermally degraded branched PPs plotted as the function of reduced extensional strain rate, $a_T \dot{\epsilon}$. Here a_T stands for the horizontal Arrhenius shift factor

It has been found that the utilized Generalized Newtonian law [159 – 161], modified White Metzner model [162], Yao model [163] and Extended Yao model [164] have the capability to describe the measured steady state shear and extensional rheology of the virgin as well as degraded branched PPs. Analysis of the rheological data via the utilized model parameters has revealed that, firstly, the model macroscopic relaxation time plotted as the function of degradation

time has been found to follow the same non-monotonic trend with local maximum at 5 h (see Figure 29), which was observed experimentally in basic shear flow and molecular weight characteristics (M_w/M_n , M_z , M_{z+1}); Secondly, it has been found that the strain hardening parameter ζ in the Generalized Newtonian model, strain hardening λ_0/K_2 parameter in the modified White Metzner model as well as μ_s/η_0 parameter in the Yao model and the ceiling stretch for disentanglement S_0 in the extended Yao model follows the non-monotonic trend in the extensional strain hardening level with respect to degradation time as observed experimentally, i.e., all four models were found to have the capability to quantify the level of the branching for virgin as well as degraded PPs. Interestingly, Yao and Generalized Newtonian models showed the capability to quantify level of extensional strain hardening (i.e., the maximum steady-state uniaxial extensional viscosity divided by three-fold Newtonian viscosity) as a function of degradation time not only quantitatively but also qualitatively. Finally, based on the Yao's μ_s/η_0 parameter (characterizing the resistance against the slip of the coil), it was suggested that the local maximum at 5 h in shear rheological characteristics and molecular weight could be explained by the presence of high molecular weight branches. On the other hand, the local minimum in shear rheology characteristics and molecular weights with simultaneous occurrence of maximum in extensional strain hardening observed at 3 h of thermal degradation was suggested to be due to the presence of a high number of short branches. Simplified visualization of possible changes in “characteristic” star polymer coil during thermal degradation according to collected experimental data and the above-described hypothesis is provided in Figure 31. Here, the coil size is proportional to the molecular weight, the longest branches are represented by the green colour, and branches formed via branch scission and recombination reactions are represented here by blue/purple and brown colours, respectively. It should also be mentioned that the presented image of molecular changes during thermal degradation of branched PP is consistent with the Bueche degradation theory and conclusions from [106], i.e., that the longest chains break first.

THERMAL DEGRADATION

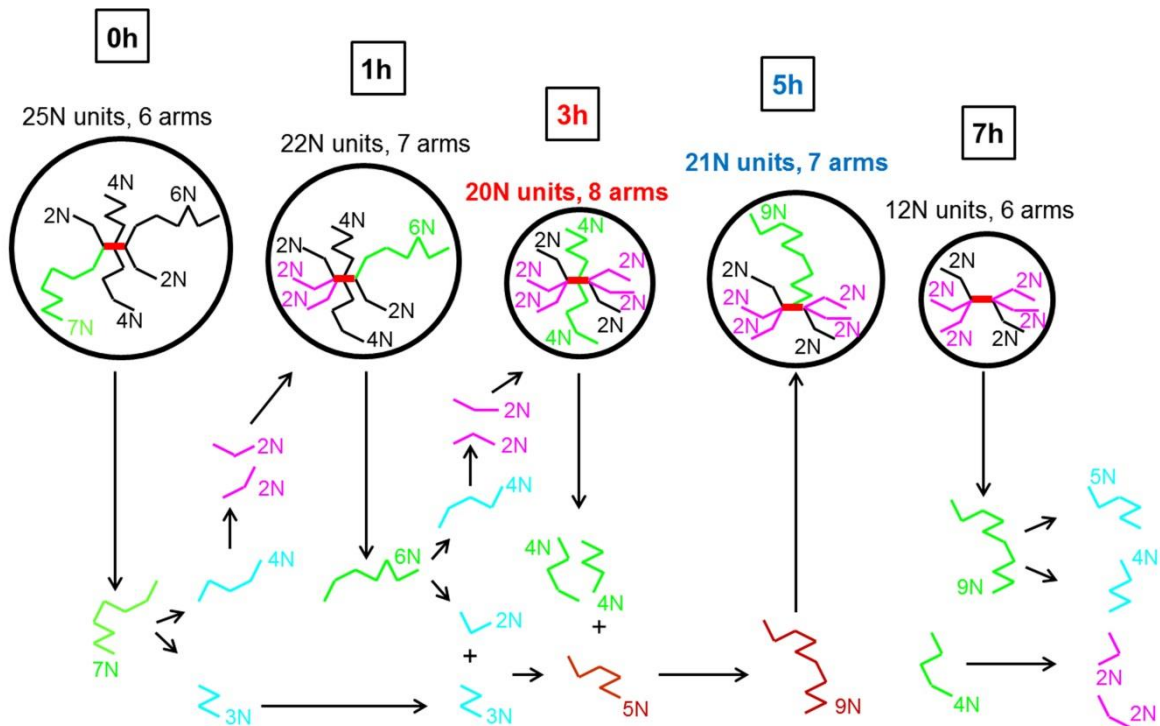


Fig. 31: Simplified visualization of possible changes in “characteristic” polymer coil for investigated branched PP (Daploy WB180HMS) at 180 °C during thermal degradation

Rheological characterization of linear Borflow polypropylenes (L-PP) [Paper II]

Three linear MB isotactic PPs, with weight average molecular weights between 56,250 – 75,850 g/mol, have been characterized over a very wide shear strain rate range ($10 - 10^7 \text{ s}^{-1}$). A primary Newtonian plateau, pseudoplastic region and well developed secondary Newtonian plateau were identified for all PP melts (see example for the medium molecular weight PP in Figure 32). Based on the estimated pressure sensitivity coefficient, $\beta = 20.00 \text{ GPa}^{-1}$, which is typical value for PP melts [165], it was deduced that the effect of viscous dissipation and pressure is mutually cancelled, i.e. that the measured viscosity data can be considered as the true material property within whole applied shear rate range.

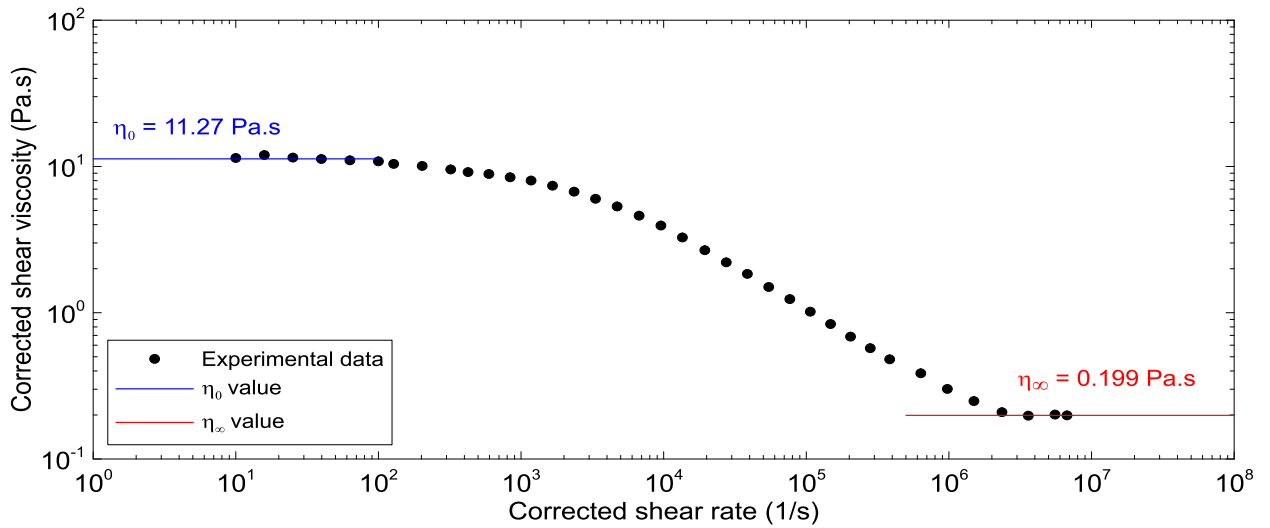


Fig. 32: Deformation rate dependent shear viscosity data for linear isotactic PP Borflow 64k at 230 °C

The measured flow curves were fitted by six different viscosity models. Two modified models, namely a modified Carreau and a Quemada model were developed. It has been found that the shear flow data could be more accurately described over the wide strain rate range by the newly suggested models. As the example, Figure 33 shows comparison between conventional and modified Carreau model fits for the medium molecular weight PP melt. The accuracy of curve fitting was found to be decreased in the following order: Modified Quemada model [166], Modified Carreau model [166], Carreau-Yasuda model [167], Cross model [168], Generalized Quemada model [169, 170] and Carreau model [171].

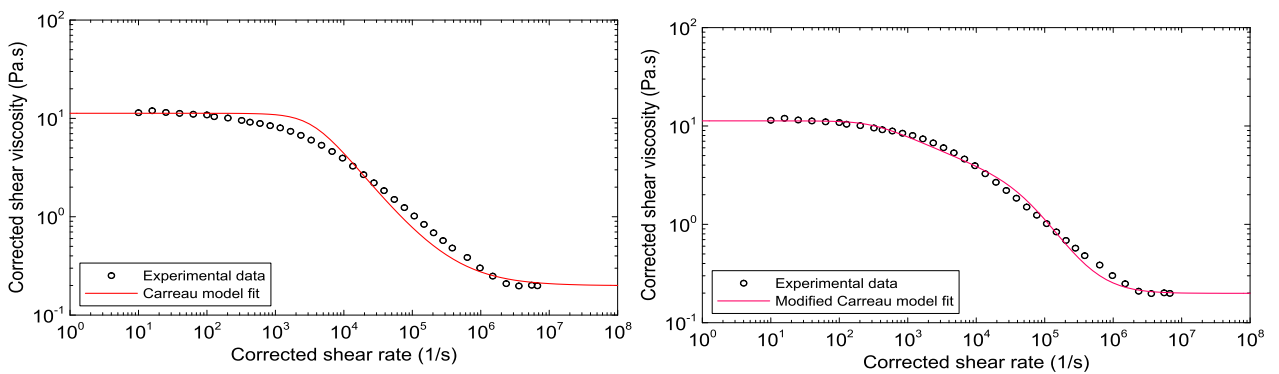


Fig. 33: Comparison between experimentally determined shear viscosity data and predictions of original (left) and modified Carreau model (right) for linear isotactic PP Borflow 64k sample at 230 °C and fixed η_0 and η_∞ parameters

One may consider under what circumstances are proposed modified models more desirable than the conventional models? One of the key reason for going to modified models are their improved flexibility do describe experimental data, especially at the high shear rate range. For example, the Cross model showed over prediction in shear viscosity by 12 % (average) – 26 % (maximum deviation) at shear rates between $1.2 \times 10^5 \text{ s}^{-1}$ and $6.73 \times 10^6 \text{ s}^{-1}$ for given PPs and temperature. Consequently, when trying to predict the pressure drop in capillary flows for the given materials and processing conditions utilizing the Cross model, the error in the predicted pressure drop can reach 26 %, which is unacceptable considering that the experimental pressure drops can be in order of tens or hundreds MPa at such high shear rates.

Effect of molecular weight, branching and temperature on dynamics of polypropylene melts at very high shear rates [Paper II and Paper III]

Dynamics of linear polypropylene (L-PP) and long-chain branched polypropylene (LCB-PP) miscible blends, having weight average molecular weight between 64 – 78 kg/mol, was investigated via high shear rate rheology at three different temperatures (190, 210 and 230 °C). Results obtained were compared with the corresponding data for L-PP. High-shear rate secondary Newtonian plateaus, η_∞ , were identified at three different temperatures for well entangled L-PPs and L-PP/LCB-PP blends above shear rates of $2 \times 10^6 \text{ s}^{-1}$. *For the first time, it has been revealed that the secondary Newtonian viscosity, η_∞ depends linearly on the weight average molecular weight, M_w as $\eta_\infty(T) = K_\infty(T) \cdot M_w$ (see Figure 34). Interestingly, the temperature dependent proportionality constant K_∞ was found to be about 10 – 20 % lower for the blend in comparison with the pure L-PP. The observed linear dependence between η_∞ and molecular weight, as predicted by Rouse-Bueche molecular theory for polymer melts with no entanglements [172, 173], strongly supports the hypothesis that chains become fully disentangled in these polymer systems at very high shear rates. In such cases the proportionality constant K_∞ is given predominantly by the geometrical parameters characterizing the size/shape of the coil, such as for example mean square radius of gyration $\langle R^2 \rangle$, and monomeric friction coefficient (ζ). Thus, lower values of K_∞ for L-PP/LCB-PP systems can be understood by the lower value of $\langle R^2 \rangle$ and ζ in comparison with pure L-PP.*

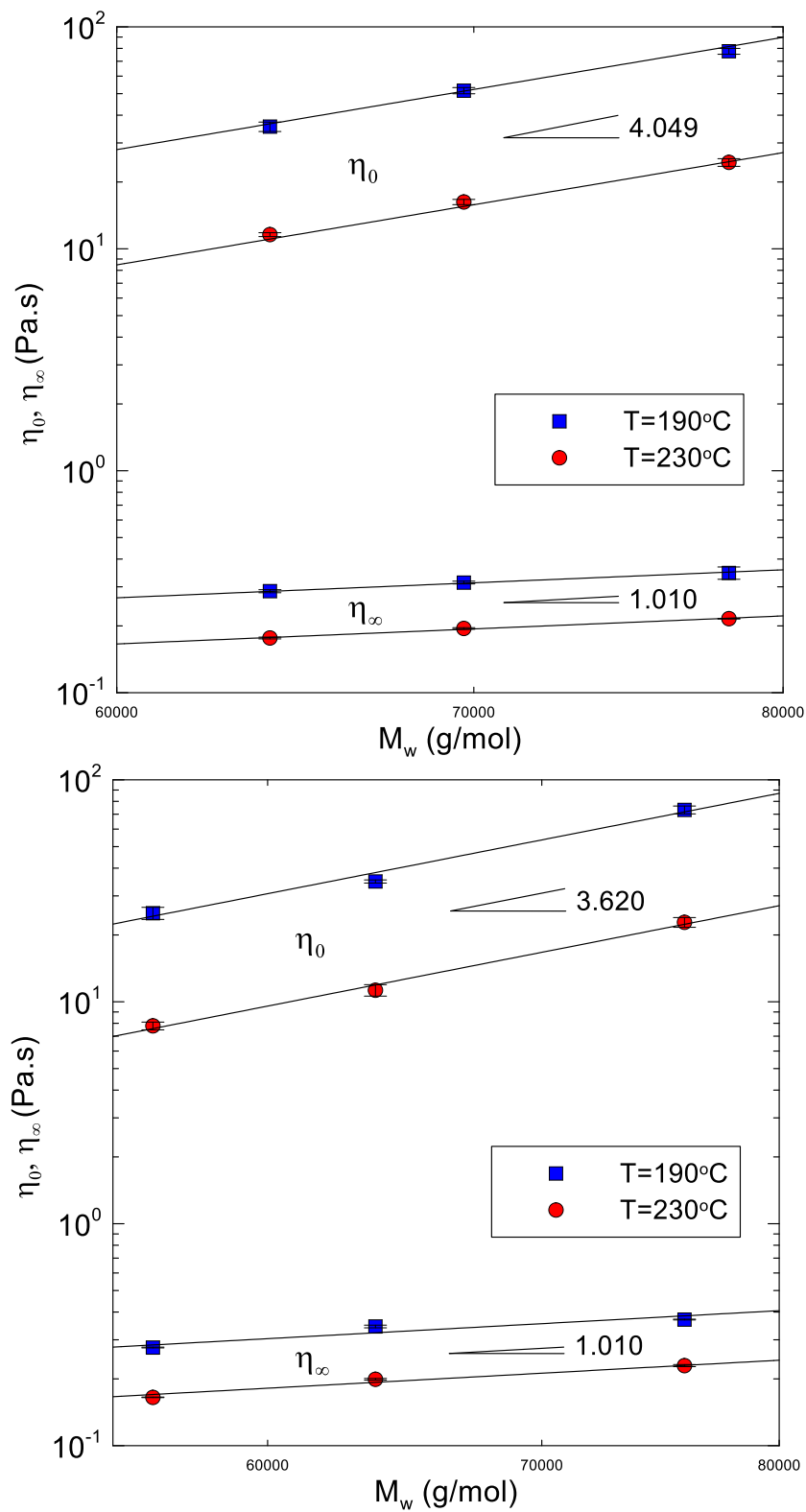


Fig. 34: Effect of weight average molecular weight, M_w , and temperature on zero shear viscosity, η_0 , and secondary Newtonian viscosity, η_∞ for L-PP/LCB-PP blends (top) and L-PP (bottom)

It has also been discovered that firstly, the high shear rate flow activation energy E_∞ for given PP melts is comparable with the flow activation energy of

PP like oligomer (squalane, $C_{30}H_{62}$; 2,6,10,15,19,23-hexamethyltetracosane) and secondly, E_{∞} , was found to be slightly lower for the blends than for pure L-PPs. This again supports the hypothesis that polymer chains are fully disentangled at very high shear rates and chain branching can enhance the flow in this regime due to smaller coil size and higher availability of the free volume (i.e. lower monomeric friction coefficient) in comparison with their linear counterparts.

To clarify the role of the chain branching on the shear viscosity at high shear rates, LCB-PP blend is compared with that of L-PP, both having the same weight average molecular weight (64 kg/mol) and comparable polydispersity index (about 4.3). In such a case, the viscosity difference is given mainly by number of entanglements, size of the macromolecular coils and ζ . As can be seen in Figure 35, the blend has an expected higher shear viscosity compared to the linear PP due to dominantly higher number of entanglements up to a shear rate of $\sim 450,000 \text{ s}^{-1}$, but above this strain rate the trend is switched.

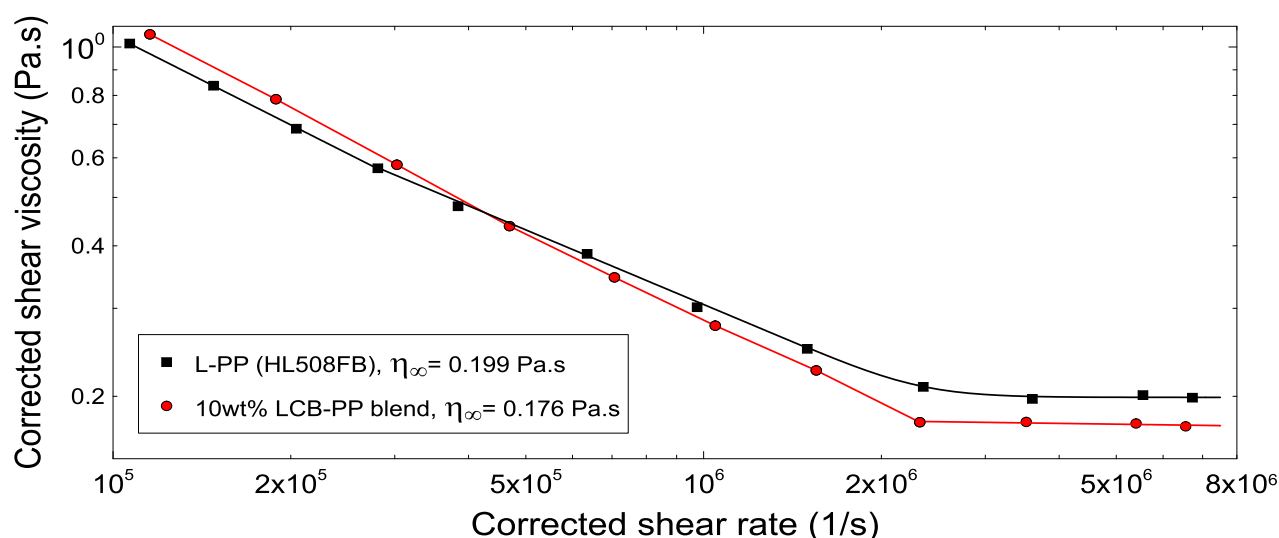


Fig. 35: Deformation rate dependent shear viscosity for LCB-PP blend and L-PP having the same molecular weight (64 kg/mol) and polydispersity index (about 4.3) at 230 °C. The term "Corrected" utilized here for shear viscosity and shear rate means that Bagley as well as Weissenberg-Rabinowitsch corrections were applied

The secondary Newtonian plateau was found to be about 13 % higher for linear PP ($\eta_{\infty} = 0.199 \pm 0.0018 \text{ Pa.s}$) in comparison with the LCB-PP blend ($\eta_{\infty} = 0.176 \pm 0.0016 \text{ Pa.s}$) at the 230 °C. In this entanglement free flow regime the observed difference in η_{∞} can primarily be attributed to smaller coils size and

higher availability of the free volume (i.e. a smaller monomeric friction coefficient) for the blend in comparison with pure linear PP melt.

Influence of long chain branching on fiber diameter distribution for polypropylene nonwovens produced by melt blown process [Paper IV]

Well characterized L-PP and LCB-PP blend samples, both having comparable M_w (76 – 78 kg/mol), zero-shear viscosity (22.8 – 24.51 Pa.s at 230 °C) and polydispersity M_w/M_n (4.41 – 4.50) were used to produce nonwovens via MB technology at constant temperature (270 °C) and two different die to collector distances (200 mm and 500 mm) in order to understand role of long chain branching on the fiber diameter distribution. Melt elasticity was evaluated via characteristic relaxation time (determined by shear viscosity data fitting by Cross [168] and Carreau-Yasuda [167] models) as well as through η_0/η_∞ ratio directly from the measured experimental data. Basic morphological characteristics of produced nonwoven samples have been determined using digital image analysis of SEM images considering three different magnifications to capture nanofibers as well as microfibers (see example for LCB-PP sample in Figure 36).

It has been found that Carreau-Yasuda relaxation time is unrealistically higher for less elastic L-PP in comparison with more elastic LCB-PP blend and power-law index remains artificially the same, practically equal to 0, for both samples. In the case of the Cross model, relaxation time for more elastic LCB-PP was correctly predicted to be higher in comparison with low elastic L-PP and power-law index was found to be 0.46 and 0.36 for L-PP and LCB-PP, respectively, which is in good correspondence with the open literature. η_0/η_∞ parameter (relaxation to retardation time ratio) estimated directly from the measured data, i.e. independently of any fitting model, was suggested to be more suitable parameter for melt elasticity quantification than the fitting model dependent characteristic relaxation time especially if flow curve shows Newtonian plateau, pseudoplastic regime as well as secondary Newtonian plateau at very high shear rates (above 10^6 s^{-1} in this case). It was found that LCB-PP sample shows higher value of η_0/η_∞ and stronger temperature dependence in comparison with L-PP at the given M_w and chosen temperature range.

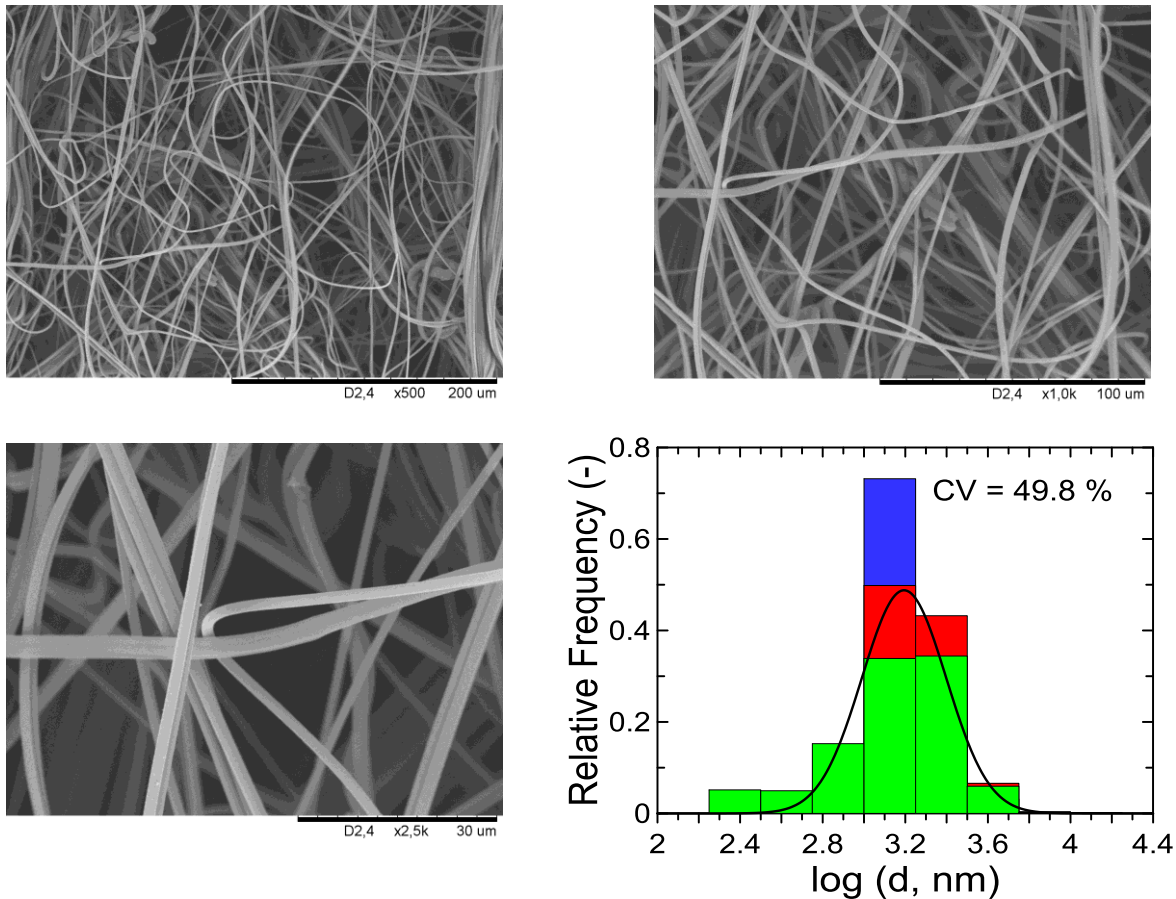


Fig. 36: SEM images for LCB-PP sample and DCD = 500 mm at two different areas and different magnifications (left – 500×, middle – 1000×, right – 2500×) together with corresponding final overall fiber diameter distribution

It has been revealed that firstly, fiber diameter distribution (coefficient of variation, *CV*) for the nonwovens produced via MB technology is lower for more elastic LCB-PP blend in comparison with less elastic L-PP sample and secondly, decrease in die to collector distance reduces *CV* (see Figure 37). Obtained results suggest, that utilization of low molecular weight and branched polymers can stabilize production of polymeric nanofibers and microfibers through MB technology considerably.

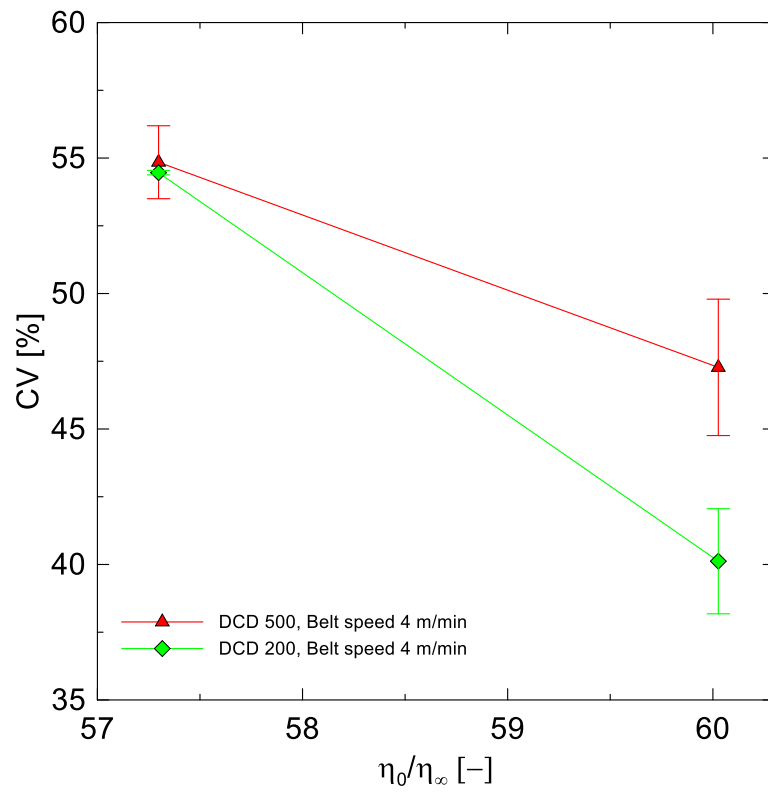


Fig. 37: Effect of η_0/η_∞ on coefficient of fiber diameter variation, CV

THE THESIS CONTRIBUTION TO SCIENCE AND PRACTICE

The most valuable contribution of the Thesis to the polymer science is discovery that high molecular weight polypropylene chains (does not matter whether they are linear or branched) become fully disentangled at the secondary Newtonian plateau region occurring above shear rates of $2 \times 10^6 \text{ s}^{-1}$. This conclusion is based on the experimentally observed linear dependency between the secondary Newtonian viscosity and molecular weight and the fact, that the high shear rate flow activation energy for given PP melts is comparable with the flow activation energy of PP like oligomer (both observations are reported here for the first time). These findings are valuable because they are changing the current view on the dynamics of polymer melts at very high deformation rates.

Observed relationships between molecular characteristics of linear and branched polypropylenes and their behavior in flows typically occurring in the melt blown technology, i.e. at very high temperatures and shear rates, as well as utilization of suggested rheological viscosity models can directly be used for the material and process optimization with respect to nanofibers production and their basic morphological characteristics. It is believed that the obtained scientific knowledge can help to understand production of polymeric nanofibers by using melt blown technology considerably as well as it can be used for development of new continuous and cheap technologies for industrial production of super-strong polypropylene fibers utilizing crystallization of flow induced disentangled melts.

CONCLUSION

In the first part of this work, the melt blown technology, which can be used to produce polymeric nanofibers, has been introduced. Specific attention has been paid to melt blown history, typical products, utilized polymers, methodologies to produce polymeric nanofibers, effect of processing conditions on basic nonwoven characteristics, flow instabilities and defects, the most frequently used polymeric materials such as linear and branched polypropylenes and high shear rate rheology.

In the second part, the complicated relationship between polymer melt rheology, molecular structure of polymers, process conditions and formation of polymeric fibers produced via melt blown technology was investigated. For such purpose, different polypropylenes (namely linear, branched and their blends) having well defined molecular architecture were chosen and rheologically characterized in very wide shear rate range utilizing different constitutive equations. Then, the chosen polypropylenes were used to produce polymeric nanofibers on the melt blown pilot plant line under different processing conditions in order to perform particular correlations. The most important research results are summarized below:

- It has been found that even if both chain scission and branching takes place during thermal degradation of the branched high molecular weight polypropylene, the melt strength (quantified via the level of extensional strain hardening) can increase at short degradation times. It was found that constitutive equations such as Generalized Newtonian law, modified White-Metzner model, Yao and Extended Yao models have the capability to describe and interpret the measured steady-state rheological data of the virgin as well as thermally degraded branched polypropylenes.
- A primary Newtonian plateau, pseudoplastic region and well developed secondary Newtonian plateau (occurring above shear rates of $2 \times 10^6 \text{ s}^{-1}$) were identified for all tested polypropylene melts and temperatures.
- Modified Carreau and a Quemada models, with higher capability to fit experimentally determined shear viscosity data than conventional viscosity models, were developed and tested.
- For the first time, it has been revealed that the secondary Newtonian viscosity, depends linearly on the weight average molecular weight, which suggests that polymer chains are fully disentangled at the secondary Newtonian plateau region. This conclusion was supported by the

experimental observation that the high shear rate flow activation energy for given PP melts is comparable with the flow activation energy of PP like oligomer (squalane, C₃₀H₆₂; 2,6,10,15,19,23-hexamethyltetracosane). It has also been deduced from the big change in the flow activation energies at low and very high shear rates that the free volume increases at the secondary Newtonian plateau due to complete chain disentanglement allowing the most probably coalescence of shaped free volume cavities.

- It was found that introduction of long-chain branching into PP, keeping the average molecular weight and polydispersity index the same, can decrease the secondary Newtonian plateau, which can primarily be attributed to smaller coils size and higher availability of the free volume (i.e. a smaller monomeric friction coefficient) for the branched PP in comparison with pure linear PP melt.
- η_0/η_∞ parameter (relaxation to retardation time ratio) estimated directly from the measured data, i.e. independently of any fitting model, was suggested to be more suitable parameter for melt elasticity quantification than the fitting model dependent characteristic relaxation time especially if flow curve shows Newtonian plateau, pseudoplastic regime as well as secondary Newtonian plateau at very high shear rates (above 10⁶ s⁻¹).
- It has been revealed that firstly, fiber diameter distribution (coefficient of variation) for the nonwovens produced via melt blown technology is lower for branched PP in comparison with linear PP sample (both having the same molecular weight and polydispersity index). Obtained results suggest, that utilization of low molecular weight and branched polymers can stabilize production of polymeric nanofibers and microfibers through melt blown technology considerably.

REFERENCES

- [1] DUTTON, K. C., Overview and analysis of the meltblown process and parameters. *Journal of Textile and Apparel, Technology and Management*. 2009, vol. 6, no. 1.
- [2] McCULLOCH, J. G., The history of the development of melt blowing technology. *International Nonwovens Journal*. 1999, vol. 8, no. 1, p. 139-149.
- [3] SHAMBAUGH, R. L., A macroscopic view of the melt-blowing process for producing microfibers. *Industrial and Engineering Chemistry Research*. 1988, vol. 27, no. 12, p. 2363-2372.
- [4] GAHAN, R. and G. C. ZGURIS, A review of the melt blown process. *Proceeding of the Annual Battery Conference on Applications and Advances*. 2000, vol. 2000, p. 145-149.
- [5] ZHAO, R., Melt blown dies: a hot innovation spot. *International Nonwovens Journal*. 2002, vol. 11, no. 4, p. 37-41.
- [6] Scopus services. *SciVerse: Open to accelerate science* [online]. URL: <<https://www.scopus.com/home.uri>> [cit. 2018-8-7]
- [7] NAYAK, R., Fabrication and characterization of polypropylene nanofibers by melt electrospinning and meltblowing. *Ph.D. Thesis*. RMIT University, Australia, 2012.
- [8] WANG, X. and Q. KE, Experimental investigation of adhesive meltblown web production using accessory air. *Polymer Engineering and Science*. 2006, vol. 46, no. 1, p. 1-7.
- [9] BRESEE, R. R. and W. KO., Fiber formation during melt blowing. *International Nonwovens Journal*. 2003, vol. 12, no. 2, p. 21-28.
- [10] DE ROVERE, A., R. L. SHAMBAUGH and E. A. O'REAR, Investigation of gravity-spun, melt-spun, and melt-blown polypropylene fibers using atomic force microscopy. *Journal of Applied Polymer Science*. 2000, vol. 77, no. 9, p. 1921-1937.
- [11] RAO, R. S. and R. L. SHAMBAUGH, Vibration and stability in the melt blowing process. *Industrial and Engineering Chemistry Research*. 1993, vol. 32, no. 12, p. 3100-3111.
- [12] CHEN, T., C. ZHANG, X. CHEN and Q. LI, Numerical computation of the fiber diameter of melt blown nonwovens produced by the inset die. *Journal of Applied Polymer Science*. 2009, vol. 111, no. 4, p. 1775-1779.
- [13] TAN, D. H., C. ZHOU, C. J. ELLISON, S. KUMAR, C. W. MACOSKO and F. S. BATES, Meltblown fibers: influence of viscosity and elasticity

- on diameter distribution. *Journal of Non-Newtonian Fluid Mechanics*. 2010, vol. 165, no. 15-16, p. 892-900.
- [14] XIN, S. and X. WANG, Shear flow of molten polymer in melt blowing. *Polymer Engineering and Science*. 2012, vol. 52, no. 6, p. 1325-1331.
- [15] WARD, G. F., Meltblown nanofibers for nonwoven filtration applications. *Filtration and Separation*. 2001, vol. 38, no. 9, p. 42-43.
- [16] Google Patents [online]. [viewed 2018-08-12]. Available from: <https://patents.google.com/>
- [17] BHAT, G. S. and S. R. MALKAN, Polymer-laid web formation. In: *Handbook of nonwovens*, RUSSELL S. J., Woodhead publishing in textiles. Cambridge, England: CRC Press, 2007, 143-195. ISBN 978-1-85573-603-0
- [18] KAREEM, S. A., Meltblown web technology: process and applications. *Journal of Engineering Applications*. 2000, vol. 2, no. 1, p. 24-34.
- [19] KEENE, B., M. BOURHAM, V. VISWANATH, H. AVCI and R. KOTEK, Characterization of degradation of polypropylene nonwovens irradiated by γ -ray. *Journal of Applied Polymer Science*. 2014, vol. 131, no. 4, article number 39917.
- [20] SOLTANI, I. and C. W. MACOSKO, Influence of rheology and surface properties on morphology of nanofibers derived from islands-in-the-sea meltblown nonwovens. *Polymer (United Kingdom)*. 2018, vol. 145, p. 21-30.
- [21] DAS, D., A. K. PRADHAN, R. CHATTOPADHYAY and S. N. SINGH, Composite nonwovens. *Textile Progress*. 2012, vol. 44, no. 1, p. 1-84.
- [22] WANG, H., Y. ZHANG, H. GAO, X. JIN and X. XIE, Composite meltblown nonwoven fabrics with large pore size as Li-ion battery separator. *International Journal of Hydrogen Energy*. 2016, vol. 41, no. 1, p. 324-330.
- [23] ZHAO, J., C. XIAO, N. XU, Evaluation of polypropylene and poly (butylmethacrylate-co-hydroxyethylmethacrylate) nonwoven material as oil absorbent. *Environmental Science and Pollution Research*. 2013, vol. 20, no. 6, p. 4137-4145.
- [24] ERBEN, J., K. PILAROVA, F. SANETRNIK, J. CHVOJKA, V. JENCOVA, L. BLAZKOVA, J. HAVLICEK, O. NOVAK, P. MIKES, E. PROSECKA, D. LUKAS and E. KUZELOVA KOSTAKOVA, The combination of meltblown and electrospinning for bone tissue engineering. *Materials Letters*. 2015, vol. 143, p. 172-176.

- [25] GUTAROWSKA, B. and A. MICHALSKI, Antimicrobial activity of filtrating meltblown nonwoven with the addition of silver ions. *Fibres and Textiles in Eastern Europe*. 2009, vol. 74, no. 3, p. 23-28.
- [26] LIU, Y., B. CHENG, N. WANG, W. KANG, W. ZHANG, K. XING and W. YANG, Development and performance study of polypropylene/polyester bicomponent melt-blowns for filtration. *Journal of Applied Polymer Science*. 2012, vol. 124, no. 1, p. 296-301.
- [27] HASSAN, M. A., B. Y. YEOM, A. WILKIE, B. POURDEYHIMI and S. A. KHAN, Fabrication of nanofiber meltblown membranes and their filtration properties. *Journal of Membrane Science*. 2013, vol. 427, p. 336-344.
- [28] GRAFE, T. and K. GRAHAM, Polymeric nanofibers and nanofiber webs: a new class of nonwovens. *International Nonwovens Technical Conference, TAPPI Conference*, 2002.
- [29] ELLISON, C. J., A. PHATAK, D. W. GILES, C. W. MACOSKO and F. S. BATES, Melt blown nanofibers: fiber diameter distributions and onset of fiber breakup. *Polymer*. 2007, vol. 48, no. 11, p. 3306-3316.
- [30] NAYAK, R., I. L. KYRATZIS, Y. B. TRUONG, R. PADHYE, L. ARNOLD, G. PEETERS, M. O'SHEA and L. NICHOLS, Fabrication and characterization of polypropylene nanofibres by meltblowing process using different fluids. *Journal of Materials Science*. 2013, vol. 48, no. 1, p. 273-281.
- [31] ZUO, F., D. H. TAN, Z. WANG, S. JEUNG, C. W. MACOSKO and F. S. BATES, Nanofibers from melt blown fiber-in-fiber polymer blends. *ACS Macro Letters*. 2013, vol. 2, no. 4, p. 301-305.
- [32] WANG, Z., X. LIU, C. W. MACOSKO and F. S. BATES, Nanofibers from water-extractable melt-blown immiscible polymer blends. *Polymer (United Kingdom)*. 2016, vol. 101, p. 269-273.
- [33] BRANG, J., A. WILKIE and J. HAGGARD, Method and apparatus for production of meltblown nanofibers. US Patent 2008/0023888.
- [34] NAYAK, R., R. PADHYE, I. L. KYRATZIS, Y. B. TRUONG and L. ARNOLD, Recent advances in nanofibre fabrication techniques. *Textile Research Journal*. 2012, vol. 82, no. 2, p. 129-147.
- [35] WILSON, A., The formation of dry, wet, spunlaid and other types of nonwovens. In: Applications of nonwovens in technical textiles, CHAPMAN, R. A., *Woodhead publishing series in textiles*. Cambridge, England: CRC Press, 2010, 3-16. ISBN 978-1-84569-437-1

- [36] WILKIE, A. and J. HAGGARD, Nanofiber melt blown nonwovens-A new low. *International Fiber Journal*. 2007, vol. 22, no. 3, p. 48-49.
- [37] CHEN, T., L., LI and X. HUANG, Fiber diameter of polybutylene terephthalate melt-blown nonwovens. *Journal of Applied Polymer Science*. 2005, vol. 97, p. 1750-1752.
- [38] CHEN, T., X., WANG and X. HUANG, Effects of processing parameters on the fiber diameter of melt blown nonwoven fabrics. *Textiles Research Journal*. 2005, vol. 75, no. 1, p. 76-80.
- [39] CHEN, T. and X. HUANG, Air drawing of polymers in the melt blowing nonwoven process: mathematical modeling. *Modeling And Simulation In Materials Science and Engineering*. 2004, vol. 12, no. 3, p. 381-388.
- [40] CHEN, T. and X. HUANG, Modeling polymer air drawing in the melt blowing nonwoven process, *Textile Research Journal*. 2003, vol. 73, no. 7, p. 651-654.
- [41] CHEN, T., X., WANG and X. HUANG, Modeling the air-jet flow field of a dual slot die in the melt blowing nonwoven process, *Textile Research Journal*. 2004, vol. 74, no. 11, p. 1018-1024.
- [42] WU, L. L., D. H., HUANG and T. CHEN, Modeling the nanofiber fabrication with the melt blowing annular die, *Revista Matéria*. 2014, vol. 19, no. 4, p. 377-381.
- [43] BRESEE, R. R. and U. A. QURESHI, Influence of process conditions on melt blown web structure: Part IV – fiber diameter. *Journal of Engineered Fibers and Fabrics*. 2006, vol. 1, no. 1, p. 32-46.
- [44] KAYSER, J. C. and R. L. SHAMBAUGH, The manufacture of continuous polymeric filaments by the melt-blowing process. *Polymer Engineering and Science*. 1990, vol. 30, no. 19, p. 1237-1251.
- [45] UYTENDAELE, M. A. J. and R. L. SHAMBAUGH, Melt blowing: General equation development and experimental verification. *American Institute of Chemical Engineers Journal*. 1990, vol. 36, no. 2, p. 175-186.
- [46] TYAGI, M. K. and R. L. SHAMBAUGH, Use of oscillating gas jets in fiber processing. *Industrial and Engineering Chemistry Research*. 1995, vol. 34, p. 656-660.
- [47] MOORE, E. M., D. V., PAPAVASSILIOU and R. L. SHAMBAUGH, Air velocity, air temperature, fiber vibration and fiber diameter measurements on a practical melt blowing die. *International Nonwovens Journal*. 2004, vol. 13, no. 3, p. 43-53.

- [48] MARLA, V. T. and R. L. SHAMBAUGH, Three-Dimensional model of the melt-blowing process, *Industrial and Engineering Chemistry Research*. 2003, vol. 42, no. 26, p. 6993-7005.
- [49] MARLA, V. T. and R. L. SHAMBAUGH, Modeling of the melt blowing performance of slot die, *Industrial and Engineering Chemistry Research*. 2004, vol. 43, no. 11, p. 2789-2797.
- [50] SHAMBAUGH, B. R., D. V. PAPAVALASSILIOU and R. L. SHAMBAUGH, Next-generation modeling of melt blowing, *Industrial and Engineering Chemistry Research*. 2011, vol. 50, p. 12233-12245.
- [51] STRAEFFER, G. and B. C. GOSWAMI, Mechanical and structural properties of melt-blown fibers. In J. E. Riedel (Ed.), *Principles of nonwovens*, 1992, Cary, NC: INDA, p. 479-513.
- [52] WADSWORTH, L. C. and A. M. JONES, Novel melt blown research findings. *The International Nonwovens Technical Conference*. Philadelphia, USA, 1986, code 11191.
- [53] CHOI, K. J., J. E. SPRUIELL, J. F. FELLERS and L. C. WADSWORTH, Strength properties of melt blown nonwoven webs, *Polymer Engineering and Science*. 1988, vol. 28, no. 2, p. 81-89.
- [54] LEE, Y. and L. C. WADSWORTH, Structure and filtration properties of melt blown polypropylene webs, *Polymer Engineering and Science*. 1990, vol. 30, no. 22, p. 1413-1419.
- [55] MILLIGAN, M. W., F. LU, R. R. BUNTIN and L. C. WADSWORTH, The use of crossflow to improve nonwoven melt-blown fibers, *Journal of Applied Polymer Science*. 1992, vol. 44, p. 279-288.
- [56] SUN, Q., D. ZHANG, B. CHEN and L. C. WADSWORTH, Application of neural network to meltblown process control, *Journal of Applied Polymer Science*. 1996, vol. 62, p. 1605-1611.
- [57] WENTE, V. A., E. L. BOONE and C. D. FLUHARTY, Manufacture of superfine organics fibers, (NRL Report 4364), 1954, Washington, D. C.: Naval Research Laboratory.
- [58] ZHANG, D., C., SUN, J. BEARD, H. BROWN, I. CARSON and C. HWO, Development and characterization of poly(trimethylene terephthalate)- based bicomponents meltblown nonwovens, *Journal of Applied Polymer Science*. 2002, vol. 83, p. 1280-1287.
- [59] YESIL, Y. and G. S. BHAT, Structure and mechanical properties of polyethylene melt blown nonwovens, *International Journal of Clothing Science and Technology*. 2016, vol. 28, no. 6, p. 780-793.

- [60] HAYES, B. D., An experimental and analytical investigation on the production of microfibers using a single-hole melt blowing process, Ph.D Thesis. The University of Tennessee, Knoxville, USA, 1991.
- [61] KHAN, A. Y. A., A fundamental investigation of the effects of die geometry and process variables on fiber diameter and quality of melt blown polypropylene webs, *Ph.D Thesis*. The University of Tennessee, Knoxville, USA, 1993.
- [62] MALKAN, S. R., Process-structure-property relationships in different molecular weight polypropylene melt-blown webs, *Ph.D Thesis*. The University of Tennessee, Knoxville, USA, 1990.
- [63] FENG, J., Preparation and properties of poly(lactic acid) fiber melt blown non-woven disordered mats, *Materials Letters*. 2017, vol. 189, p. 180-183.
- [64] GUO, M., H. LIANG, Z. LUO, Q. CHEN and W. WEI, Study on melt-blown processing, web structure of polypropylene nonwovens and its BTX adsorption, *Fibers and Polymers*. 2016, vol. 17, no. 2, p. 257-265.
- [65] RENUKARN, R., W. TAKARADA and T. KIKUTANI, Melt-blowing conditions for preparing webs consisting of fine fibers, *AIP Conference Proceedings*. 2016, vol. 1779, art. n. 120002.
- [66] JARECKI, L., A. ZIABICKI, Z. LEWANDOWSKI and A. BLIM, Dynamics of air drawing in the melt blowing of nonwovens from isotactic polypropylene by computer modeling, *Journal of Applied Polymer Science*. 2011, vol. 119, no. 1, p. 53-65.
- [67] WANG, Y. and X. WANG, Investigation on a New Annular Melt-Blowing die using numerical simulation, *Industrial and Engineering Chemistry Research*. 2013, vol. 52, no. 12, p. 4597-4605.
- [68] ZENG, Y. C., Y. F. SUN and X. H. WANG, Numerical approach to modeling fiber motion during melt blowing, *Journal of Applied Polymer Science*. 2011, vol. 119, no. 4, p. 2112-2123.
- [69] NAYAK, R., I. L. KYRATZIS, Y. B. TRUONG, R. PADHYE and L. ARNOLD, Structural and mechanical properties of polypropylene nanofibres fabricated by meltblowing, *Journal of the Textile Institute*. 2015, vol. 106, no. 6, p. 629-640.
- [70] BRESEE, R. R. and U. A. QURESHI, Influence of processing conditions on melt blown web structure: Part 1 – DCD, *International Nonwovens Journal*. 2004, vol. 13, no. 1, p. 49-55.
- [71] BRESEE, R. R., U. A. QURESHI and M. C. PELHAM, Influence of processing conditions on melt blown web structure: Part 2 – Primary

- airflow rate, *International Nonwovens Journal*. 2005, vol. 14, no. 2, p. 11-18.
- [72] WU, T. T. and R. L. SHAMBAUGH, Characterization of the melt blowing process with laser Doppler velocimetry, *Industrial and Engineering Chemistry Research*. 1992, vol. 31, p. 379-389.
- [73] UPPAL, R., G. BHAT, C. EASH and K. AKATO, Meltblown nanofiber media for enhanced quality factor, *Fibers and Polymers*. 2013, vol. 14, no. 4, p. 660-668.
- [74] QURESHI, U. A., Understanding the role of the collector during melt blowing, *Master Thesis*. The University of Tennessee, Knoxville, USA, 2001.
- [75] GHOSAL, A., S. SINHA-RAY, L. A. YARIN and B. POURDEYHIMI, Numerical prediction of the effect of uptake velocity on three-dimensional structure, porosity and permeability of meltblown nonwoven laydown, *Polymer (United Kingdom)*. 2016, vol. 85, p. 19-27.
- [76] ZAPLETALOVA, T., S. MICHELSEN and B. POURDEYHIMI, Polyether based thermoplastic polyurethane melt blown nonwovens, *Journal of Engineered Fibers and Fabrics*. 2006, vol. 1, no. 1, p. 62-72.
- [77] XIE, S., Y. ZHENG and Y. ZENG, Influence of die geometry on fiber motion and fiber attenuation in the melt-blowing process. *Industrial and Engineering Chemistry Research*. 2014, vol. 53, no. 32, p. 12866-12871.
- [78] CHHABRA, R. and R. L. SHAMBAUGH, Experimental measurements of fiber threadline vibrations in the melt-blowing process. *Industrial and Engineering Chemistry Research*. 1996, vol. 35, no. 11, p. 4366-4374.
- [79] HAN, W. and X. WANG, Modeling melt blowing fiber with different polymer constitutive equations. *Fibers and Polymers*. 2016, vol. 17, no. 1, p. 74-79.
- [80] BEARD, J. H., R. L. SHAMBAUGH, B. R. SHAMBAUGH and D. W. SCHMIDTKE, On-line measurement of fiber-motion during melt blowing. *Industrial and Engineering Chemistry Research*. 2007, vol. 46, no. 22, p. 7340-7352.
- [81] XIE, S. and Y. ZENG, Online measurement of fiber whipping in the melt-blowing process. *Industrial and Engineering Chemistry Research*. 2013, vol. 52, no. 5, p. 2116-2122.
- [82] SUN, Y., Y. ZENG and X. WANG, Three-dimensional model of whipping motion in the processing of microfibers. *Industrial and Engineering Chemistry Research*. 2011, vol. 50, no. 2, p. 1099-1109.

- [83] XIE, S. and Y. ZENG, Turbulent air flow field and fiber whipping motion in the melt blowing process: Experimental study. *Industrial and Engineering Chemistry Research*. 2012, vol. 51, no. 14, p. 5346-5352.
- [84] CHUNG, C. and S. KUMAR, Onset of whipping in the melt blowing process. *Journal of Non-Newtonian Fluid Mechanics*. 2013, vol. 192, p. 37-47.
- [85] XIE, S., W. HAN, G. JIANG and C. CHEN, Turbulent air flow field in slot-die melt blowing for manufacturing microfibrinous nonwoven materials. *Journal of Materials Science*. 2018, vol. 53, no. 9, p. 6991-7003.
- [86] MUSIL, J. and M. ZATLOUKAL, Historical review of die drool phenomenon in plastic extrusion. *Polymer Reviews*. 2014, vol. 54, no. 1, p. 139-184.
- [87] MUSIL, J. and M. ZATLOUKAL, Experimental investigation of flow induced molecular weight fraction phenomenon for two linear HDPE polymer melts having same M_n and M_w but different M_z and M_{z+1} average molecular weights. *Chemical Engineering Science*. 2012, vol. 81, p. 146-156.
- [88] BRESEE, R. R. and U. A. Qureshi, Fiber motion near the collector during melt blowing: part 2 – fly formation. *International Nonwovens Journal*. 2002, vol. 11, no. 3, p. 21-27.
- [89] HAN, W., G. S. BHAT and X. WANG, Investigation of nanofiber breakup in the melt-blowing process. *Industrial and Engineering Chemistry Research*. 2016, vol. 55, no. 11, p. 3150-3156.
- [90] PINCHUK, L.S., V. A. GOLDADE, A. V. MAKAREVICH and V. N. KESTELMAN, Melt blowing techniques. In: Melt blowing equipment, technology, and polymer fibrous materials, PINCHUK, L. S., V. A. GOLDADE, A. V. MAKAREVICH and V. N. KESTELMAN, *Materials processing*. New York, USA: Springer, 2002, 5-20, ISBN 3-540-43223-x
- [91] VARGAS, E., Meltblown technology Today: an overview of raw materials, processes, products, markets, and emerging end uses. San Francisco, USA: California: Miller Freeman, 1989, 1-316, ISBN 9780879301767
- [92] TAN, D. H., P. K. HERMAN, F. S. BATES, S. KUMAR and C. W. MACOSKO, Influence of Laval nozzles on the air flow field in melt blowing apparatus. *Chemical Engineering Science*. 2012, vol. 80, p. 342-348.
- [93] MAJCHRZYCKA, K., M. OKRASA, A. BROCHOCKA and W. URBANIAK-DOMAGALA, Influence of low-temperature plasma

- treatment on the liquid filtration efficiency of melt-blown PP nonwovens in the conditions of simulated use of respiratory protective equipment. *Chemical and Process Engineering-Inzynieria Chemiczna I Procesowa*. 2017, vol. 38, no. 2, p. 195-207.
- [94] KO, W. C. and R.R. BRESEE, FT-IR microspectroscopic study of shot formation in melt-blown webs. *Applied Spectroscopy*. 2003, vol. 57, no. 6, p. 636-641.
- [95] BRESEE, R. R., Influence of processing conditions on melt blown web structure. Part III – water quench. *International Nonwovens Journal*. 2005, vol. 14, no. 4, p. 27-35.
- [96] ZHOU, C., D. H. TAN, A. P. JANAKIRAMAN and S. KUMAR, Modeling the melt blowing of viscoelastic materials. *Chemical Engineering Science*. 2011, vol. 66, no. 18, p. 4172-4183.
- [97] TZOGANAKIS, C., J. VLACHOPOULOS and A. E. HAMIELEC, Production of controlled-rheology polypropylene resins by peroxide promoted degradation during extrusion. *Polymer Engineering & Science*. 1988, vol. 28, no. 3, p. 170-180.
- [98] TZOGANAKIS, C., A. E. HAMIELEC, Y. TANG and J. VLACHOPOULOS, Controlled degradation of polypropylene: a comprehensive experimental and theoretical investigation. *Polymer-Plastics Technology and Engineering*. 1989, vol. 28, no. 3, p. 319-350.
- [99] TZOGANAKIS, C., J. VLACHOPOULOS, A. E. HAMIELEC and D. M. SHINOZAKI, Effect of molecular weight distribution on the rheological and mechanical properties of polypropylene. *Polymer Engineering & Science*. 1989, vol. 29, no. 6, p. 390-396.
- [100] MACHADO, A. V., J. A. COVAS and M. VAN DUIN, Monitoring polyolefin modification along the axis of a twin screw extruder. I. effect of peroxide concentration. *Journal of Applied Polymer Science*. 2001, vol. 81, no. 1, p. 58-68.
- [101] VAN DUI, M., A. V. MACHADO and J. COVAS, A look inside the extruder: evolution of chemistry, morphology and rheology along the extruder axis during reactive processing and blending. *Macromolecular Symposia*. 2001, vol. 170, p. 29-39.
- [102] MACHADO, A. V., J. M. MAIA, S. V. CANEVAROLO and J. A. COVAS, Evolution of peroxide-induced thermomechanical degradation of polypropylene along the extruder. *Journal of Applied Polymer Science*. 2004, vol. 91, no. 4, p. 2711-2720.

- [103] BERZIN, F., B. VERGNES, S. V. CANEVAROLO, A. V. MACHADO and J. A. COVAS, Evolution of the peroxide-induced degradation of polypropylene along a twin-screw extruder: experimental data and theoretical predictions. *Journal of Applied Polymer Science*. 2006, vol. 99, no. 5, p. 2082-2090.
- [104] HINSKEN, H., S. MOSS, J. R. PAUQUET and H. ZWEIFEL, Degradation of polyolefins during melt processing. *Polymer Degradation and Stability*. 1991, vol. 34, no. 1-3, p. 279-293.
- [105] GONZALEZ-GONZALEZ, V. A., G. NIERA-VELAZQUEZ and J. L. ANGULO-SANCHEZ, Polypropylene chain scissions and molecular weight changes in multiple extrusion. *Polymer Degradation and Stability*. 1998, vol. 60, no. 1, p. 33-42.
- [106] CANEVAROLO, S. V., Chain scission distribution function for polypropylene degradation during multiple extrusions. *Polymer Degradation and Stability*. 2000, vol. 70, no. 1, p. 71-76.
- [107] WALDMAN, W. R. and M. A. DE PAOLI, Thermo-mechanical degradation of polypropylene, low-density polyethylene and their 1:1 blend. *Polymer Degradation and Stability*. 1998, vol. 60, no. 2-3, p. 301-308.
- [108] DROZDOV, A. D., The effect of thermal oxidative degradation of polymers on their viscoelastic response. *International Journal of Engineering Science*. 2007, vol. 45, no. 11, p. 882-904.
- [109] QUIAN, S., T. IGARASHI and K. H. NITTA, Thermal degradation behavior of polypropylene in the melt state: molecular weight distribution changes and chain scission mechanism. *Polymer Bulletin*. 2011, vol. 67, no. 8, p. 1661-1670.
- [110] LUGAO, A. B., H. OTAGURO, F. D. PARRA, A. YOSHIGA, L. F. C. P. LIMA, B. W. H. ARTEL and S. LIBERMAN, Review on the production process and uses of controlled rheology polypropylene-Gamma radiation versus electron beam processing. *Radiation Physics and Chemistry*. 2007, vol. 76, no. 11-12, p. 1688-1690.
- [111] ABBAS MOUSAVI, A., S. DADBIN, M. FROUNCHI, D. C. VENERUS and T. G. MEDINA, Comparison of rheological behavior of branched polypropylene prepared by chemical modification and electron beam irradiation under air and N₂. *Radiation Physics and chemistry*. 2010, vol. 79, no. 10, p. 1088-1094.
- [112] KRAUSE, B., D. VOIGT, A. LEDERER, D. AUHL and H. MUNSTEDT, Determination of low amounts of long-chain branches in polypropylene

- using a combination of chromatographic and rheological methods. *Journal of Chromatography A*. 2004, vol. 1056, no. 1-2, p. 217-222.
- [113] KRAUSE, B., M. STEPHAN, S. VOLKLAND, D. VOIGT, L. HAUBLER and H. DORSCHNER, Long-chain branching of polypropylene by electron-beam irradiation in the molten state. *Journal of Applied Polymer Science*. 2006, vol. 99, no. 1, p. 260-265.
- [114] AUHL, D., F. J. STADLER and H. MUNSTEDT, Rheological properties of electron beam-irradiated polypropylenes with different molar masses. *Rheologica Acta*. 2012, vol. 51, no. 11-12, p. 979-989.
- [115] RATZSCH, M., M. ARNOLD, E. BORSIG, H. BUCKA and N. REICHELT, Radical reactions on polypropylene in the solid state. *Progress in Polymer Science (Oxford)*. 2002, vol. 27, no. 7, p. 1195-1282.
- [116] AUHL, D., F. J. STADLER and H. MUNSTEDT, Comparison of molecular structure and rheological properties of electron-beam and gamma-irradiated polypropylene. *Macromolecules*. 2012, vol. 45, no. 4, p. 2057-2065.
- [117] YOSHIGA, A., H. OTAGURO, D. F. PARRA, L. F. C. P. LIMA and A. B. LUGAO, Controlled degradation and crosslinking of polypropylene induced by gamma radiation and acetylene. *Polymer Bulletin*. 2009, vol. 63, no. 3, p. 397-409.
- [118] LUGAO, A. B., B. HUTZLER, T. OJEDA, S. TOKUMOTO, R. SIEMENS, K. MAKUUCHI and A. L. C. H. VILLAVICENCIO, Reaction mechanism and rheological properties of polypropylene irradiated under various atmospheres. *Radiation Physics and Chemistry*. 2000, vol. 57, no. 3-6, p. 389-392.
- [119] HE, G. and C. TZOGANAKIS, A UV-initiated reactive extrusion process for production of controlled-rheology polypropylene. *Polymer Engineering and Science*. 2011, vol. 51, no. 1, p. 151-157.
- [120] ZAMOTAEV, P., E. SHIBIRIN and Z. NOGELLOVA, Photocrosslinking of polypropylene: the effect of different photo-initiators and coagents. *Polymer Degradation and Stability*. 1995, vol. 47, no. 1, p. 93-107.
- [121] KUKALEVA, N., K. STOLL and M. SANTI, Modified olefin polymers. US Patent 20110136931 A1.
- [122] AMINTOWLIEH, Y., C. TZOGANAKIS and A. PENLIDIS, The effect of depth and duration of UV radiation on polypropylene modification via photoinitiation. *Journal of Applied Polymer Science*. 2014, vol. 131, no. 21, article number 41021.

- [123] AMINTOWLIEH, Y., C. TZOGANAKIS, S. G. HATZIKIRIAKOS and A. PENLIDIS, Effect of processing variables on polypropylene degradation and long chain branching with UV irradiation. *Polymer Degradation and Stability*. 2014, vol. 104, no. 1, p. 1-10.
- [124] AMINTOWLIEH, Y., C. TZOGANAKIS and A. PENLIDIS, Continuous modification of polypropylene via photoinitiation. *Polymer Engineering and Science*. 2015, vol. 55, no. 10, p. 2423-2432.
- [125] AMINTOWLIEH, Y., C. TZOGANAKIS and A. PENLIDIS, Preparation and characterization of long chain branched polypropylene through UV irradiation and coagent use. *Polymer-Plastics Technology and Engineering*. 2015, vol. 54, no. 14, p. 1425-1438.
- [126] AMINTOWLIEH, Y., C. TZOGANAKIS and A. PENLIDIS, An overview of the potential of UV modification of polypropylene. *Macromolecular Symposia*. 2016, vol. 360, no. 1, p. 96-107.
- [127] PARENT, J. S., A. BODSWORTH, S. S. SENGUPTA, M. KONTOPOULOU, B. I. CHAUDHARY, D. POCHE and S. COUSTEAUX, Structure-rheology relationships of long-chain branched polypropylene: comparative analysis of acrylic and allylic coagent chemistry. *Polymer*. 2009, vol. 50, no. 1, p. 85-94.
- [128] GOTSIS, A. D., B. L. F. ZEEVENHOVEN and C. TSENOGLOU, Effect of long branches on the rheology of polypropylene. *Journal of Rheology*. 2004, vol. 48, no. 4, p. 895-914.
- [129] AUHL, D., J. STANGE, H. MUNSTEDT, B. KRAUSE, D. VOIGT, A. LEDERER, U. LAPPAN and K. LUNKWITZ, Long-chain branched polypropylenes by electron beam irradiation and their rheological properties. *Macromolecules*. 2004, vol. 37, no. 25, p. 9465-9472.
- [130] LAGENDIJK, R. P., A. H. HOGT, A. BUIJTENHUIJS and A. D. GOTSIS, Peroxydicarbonate modification of polypropylene and extensional flow properties. *Polymer*. 2001, vol. 42, no. 25, p. 10035-10043.
- [131] WONG, B. and W. E. BAKER, Melt rheology of graft modified polypropylene. *Polymer*. 1997, vol. 38, no. 11, p. 2781-2789.
- [132] YOSHII, F., K. MAKUUCHI, S. KIKUKAWA, T. TANAKA, J. SAITOH and K. KOYAMA, High-melt-strength polypropylene with electron beam irradiation in the presence of polyfunctional monomers. *Journal of Applied Polymer Science*. 1996, vol. 60, no. 4, p. 617-623.

- [133] HINGMANN, R. and B. L. MARCZINKE, Shear and elongational flow properties of polypropylene melt. *Journal of Rheology*. 1994, vol. 38, no. 3, p. 573-587.
- [134] AHIRWAL, D., S. FILIPE, I. NEUHAUS, M. BUSCH, G. SCHLATTER and M. WILHELM, Large amplitude oscillatory shear and uniaxial extensional rheology of blends from linear and long-chain branched polyethylene and polypropylene. *Journal of Rheology*. 2014, vol. 58, no. 3, p. 635-658.
- [135] RAPS, D., T. KOPPL, L. HEYMANN and V. ALTSTADT, Rheological behavior of a high-melt-strength polypropylene at elevated pressure and gas loading for foaming purposes. *Rheological Acta*. 2017, vol. 56, no. 2, p. 95-111.
- [136] DRABEK, J. and M. ZATLOUKAL, Evaluation of thermally induced degradation of branched polypropylene by using rheology and different constitutive equations. *Polymers*. 2016, vol. 8, no. 9, article number 317.
- [137] MUNSTEDT, H. and D. AUHL, Rheological measuring techniques and their relevance for the molecular characterization of polymers. *Journal of Non-Newtonian Fluid Mechanics*. 2005, vol. 128, no. 1, p. 62-69.
- [138] MUNSTEDT, H., Rheological properties and molecular structure of polymer melts. *Soft Matter*. 2011, vol. 7, no. 6, p. 2273-2283.
- [139] GABRIEL, C. and H. MUNSTEDT, Strain hardening of various polyolefins in uniaxial elongational flow. *Journal of Rheology*. 2003, vol. 47, no. 3, p. 619-630.
- [140] KOYAMA, K., M. SUGIMOTO, Rheological properties and its processability of high-melt-strength polypropylene. *In Proceedings of the XIIIth International Congress on Rheology*. Cambridge, UK, 20-25 August 2000, p. 409-410.
- [141] PARK, C. B. and L. K. CHEUNG, A study of cell nucleation in the extrusion of polypropylene foams. *Polymer Engineering and Science*. 1997, vol. 37, no. 1, p. 1-10.
- [142] SPITAEI, P. and C. W. MACOSKO, Strain hardening in polypropylenes and its role in extrusion foaming. *Polymer Engineering and Science*. 2004, vol. 44, no. 11, p. 2090-2100.
- [143] CHIKHALIKAR, K., S. BANIK, L. B. AZAD, K. JADHAV, S. MAHAJAN, Z. AHMAD, S. KULKARNI, S. GUPTA, P. DOSHI, H. POL and A. LELE, Extrusion film casting of long chain branched polypropylene. *Polymer Engineering and Science*. 2015, vol. 55, no. 9, p. 1977-1987.

- [144] KURZBECK, S., F. OSTER, H. MUNSTEDT, T. Q. NGUYEN and R. GENSLER, Rheological properties of two polypropylenes with different molecular structure. *Journal of Rheology*. 1999, vol. 43, no. 2, p. 359-374.
- [145] SUGIMOTO, M., T. TANAKA, Y. MASUBUCHI, J. I. TAKIMOTO and K. KOYAMA, Effect of chain structure on the melt rheology of modified polypropylene. *Journal of Applied Polymer Science*. 1999, vol. 73, no. 8, p. 1493-1500.
- [146] DRABEK, J., Applied rheology for melt blown rheology. *Bachelor Thesis*, Tomas Bata University in Zlin, Czech Republic. 2011.
- [147] DRABEK, J., Applied rheology for production of polypropylene nanofibers. *Master Thesis*. Tomas Bata University in Zlin, Czech Republic. 2013.
- [148] RIDES, M., A. L. KELLY and C. R. G. ALLEN, An investigation of high rate capillary extrusion rheometry of thermoplastics. *Polymer Testing*. 2011, vol. 30, no. 8, p. 916-924.
- [149] CHEN, A. F., H. X. HUANG and W. S. GUAN, Comparison of superimposed effects in high-shear-rate capillary rheometry of polystyrene, polypropylene, and linear low-density polyethylene melts. *Polymer Engineering and Science*. 2015, vol. 55, no. 3, p. 506-512.
- [150] KANG, K., L. J. LEE and K. W. KOELLING, High shear microfluidics and its application in rheological measurement. *Experiments in Fluids*. 2005, vol. 38, no. 2, p. 222-232.
- [151] KELLY, A. L., A. T. GOUGH, B. R. WHITESIDE and P. D. COATES, High shear strain rate rheometry of polymer melts. *Journal of Applied Polymer Science*. 2009, vol. 114, no. 2, p. 864-873.
- [152] FRIESENBICHLER, W., I. DURETEK, J. RAJGANESH and S. R. KUMAR, Measuring the pressure dependent viscosity at high shear rates using a new rheological injection mould. *Polimery/Polymers*. 2011, vol. 56, no. 1, p. 58-62.
- [153] MNEKBI, C., M. VINCENT and J. F. AGASSANT, Polymer rheology at high shear rate for microinjection moulding. *International Journal of Material Forming*. 2010, vol. 3, no. 1, p. 539-542.
- [154] TAKAHASHI, H., T. MATSUOKA and T. KURAUCHI, Rheology of polymer melts in high shear rate. *Journal of Applied Polymer Science*. 1985, vol. 30, no. 12, p. 4669-4684.
- [155] GUAN, W. S. and H. X. HUANG, Superimposed effects in high-shear-rate capillary rheology of polystyrene melt. *Polymer Engineering and Science*. 2013, vol. 53, no. 7, p. 1563-1570.

- [156] SENTMANAT, M. L., Miniature universal testing platform: from extensional melt rheology to solid-state deformation behavior. *Rheological Acta*. 2004, vol. 43, no. 6, p. 657-669.
- [157] Basic information about FANUC ROBOSHOT S-2000i series. URL: <<https://webbuilder3.asiannet.com/ftp/2410/FANUC%2030A.50A.100A%20spec.pdf>> [cit. 2018-8-7]
- [158] Quorum technologies preparation for excellence. URL: <<https://www.quorumtech.com/previous-products/coaters-and-evaporators>> [cit. 2018-8-7]
- [159] ZATLOUKAL, M., A simple phenomenological non-Newtonian fluid model. *Journal of Non-Newtonian Fluid Mechanics*. 2010, vol. 165, no. 11-12, p. 592-595.
- [160] ZATLOUKAL, M., Novel non-Newtonian fluid model for polymer melts. *Annual Technical Conference – ANTEC, Conference Proceedings*. 2011, vol. 1, p. 92-96.
- [161] ZATLOUKAL, M., Measurements and modeling of temperature-strain rate dependent uniaxial and planar extensional viscosities for branched LDPE polymer melt. *Polymer (United Kingdom)*. 2016, vol. 104, p. 258-267.
- [162] BARNES, H. A. and G. P. ROBERTS, A simple empirical model describing the steady-state shear and extensional viscosities of polymer melts. *Journal of Non-Newtonian Fluid Mechanics*. 1992, vol. 44, no. C, p. 113-126.
- [163] YAO, D., A non-Newtonian fluid model with an objective vorticity. *Journal of Non-Newtonian Fluid Mechanics*. 2015, vol. 218, no. April 01, p. 99-105.
- [164] YAO, D., A non-Newtonian fluid model with finite stretch and rotational recovery. *Journal of Non-Newtonian Fluid Mechanics*. 2016, vol. 230, no. April 01, p. 12-18.
- [165] SEDLACEK, T., M. ZATLOUKAL, P. FILIP, A. BOLDIZAR and P. SAHA, On the effect of pressure on the shear and elongational viscosities of polymer melts. *Polymer Engineering and Science*. 2004, vol. 44, no. 7, p. 1328-1337.
- [166] DRABEK, J., M. ZATLOUKAL and M. MARTYN, Effect of molecular weight on secondary Newtonian plateau at high shear rates for linear isotactic melt blown polypropylenes. *Journal of Non-Newtonian Fluid Mechanics*. 2018, vol. 251, p. 107-118.

- [167] YASUDA, K., R. C. ARMSTRONG and R. E. COHEN, Shear flow properties of concentrated solutions of linear and star branched polystyrenes. *Rheological Acta*. 1980, vol. 20, no. 2, p. 163-178.
- [168] CROSS, M. M., Rheology of non-Newtonian fluids: A new flow equation for pseudoplastic systems. *Journal of Colloid Science*. 1965, vol. 20, no. 5, p. 417-437.
- [169] QUEMADA, D., P. FLAUD and P. H. JEZEQUEL, Rheological properties and flow of concentrated disperse media I – Modelling of steady and unsteady behavior. *Chemical Engineering Communications*. 1985, vol. 32, no. 1-5, p. 61-83.
- [170] FANG, T., H. ZHANG, T. T. HSIEH and C. TIU, Rheological behavior of cocoa dispersions with cocoa butter replacers. *Journal of Texture Studies*. 1997, vol. 28, no. 1, p. 11-26.
- [171] CARREAU, P. J., Rheological equations from molecular network theories. *Trans Soc Rheol*. 1972, vol. 16, no. 1, p. 99-127.
- [172] BUECHE, F., Viscosity, self-diffusion, and allied effects in solid polymers. *The Journal of Chemical Physics*. 1952, vol. 20, no. 12, p. 1959-1964.
- [173] DEALY, J. M. and R. G. LARSON, In structure and rheology of molten polymers: From structure to flow behavior and back again. *Hanser Publisher*, Munich, 2006, p. 516. ISBN: 978-3-446-21771-3.

LIST OF FIGURES

<i>Fig. 1: Development of publication activity about nanofibers [6] (data taken in August 2018)</i>	<i>9</i>
<i>Fig. 2: Scheme of MB line [1, 8].....</i>	<i>10</i>
<i>Fig. 3: Visualization of fiber attenuation in post die area during MB process (left) together with particular velocity profiles in cross sections A and B (right) [14]</i>	<i>11</i>
<i>Fig. 4: Summarization of the MB die designs described in Table 1</i>	<i>13</i>
<i>Fig. 5: Spunbond-melt blown-spunbond structure [28]</i>	<i>17</i>
<i>Fig. 6: 2D fiber bending instability (left) and 3D fiber spiral motion (middle, right) [77, 81]</i>	<i>23</i>
<i>Fig. 7: Die drool phenomenon occurring during extrusion of HDPE melt through a single hole [87] (left) and during melt blowing of PP via multi hole MB die under processing conditions provided in [Paper IV] (right)....</i>	<i>24</i>
<i>Fig. 8: Fiber breakup [89].....</i>	<i>24</i>
<i>Fig. 9: Melt spraying [78].....</i>	<i>25</i>
<i>Fig. 10: Flies collected at high (left), medium (middle) and low (right) DCD [88]. The length of the black bar is 3.0 cm.....</i>	<i>25</i>
<i>Fig. 11: Visualization of isolated spherical particles on the produced mat [29, 93].....</i>	<i>26</i>
<i>Fig. 12: Damaged web due to shots (left) including detail view for one shot (right) [95]</i>	<i>26</i>
<i>Fig. 13: Jam effect [29].....</i>	<i>27</i>
<i>Fig. 14: Typical fiber diameter log-normal distribution for MB nonwoven [13].....</i>	<i>27</i>
<i>Fig. 15: Linear (left) and branched structure (right) of PP</i>	<i>28</i>
<i>Fig. 16: Three flow regimes observed in flow curves for different polymer melts [154].....</i>	<i>34</i>
<i>Fig. 17: Rotational rheometer ARES 2000</i>	<i>37</i>
<i>Fig. 18: Aluminum plate with the overflow channel.....</i>	<i>37</i>
<i>Fig. 19: Sentmanat Extensional Rheometer (SER-HV-A01)[156]</i>	<i>38</i>
<i>Fig. 20: Cross-section of twin-bore capillary rheometer</i>	<i>39</i>
<i>Fig. 21: Fanuc Roboshot S-2000i 100A [157]</i>	<i>41</i>
<i>Fig. 22: Detail view of nozzle adapter connected to injection unit</i>	<i>41</i>
<i>Fig. 23: Cross-section of assembled parts for the instruments injection molding machine</i>	<i>42</i>
<i>Fig. 24: Photo of A) orifice capillary die B) long die C) washer and D) holder utilized during high shear rate measurements.....</i>	<i>42</i>

Fig. 25: MB pilot line for two different processing conditions: (left) DCD = 500 cm, (right) DCD = 200 cm.....	43
Fig. 26: Detailed view of utilized MB die (left – side view, right – front view showing 0.4 mm diameter holes).....	43
Fig. 27: Polaron SC7640 sputtering device [158].....	44
Fig. 28: Visualization of HITACHI Tabletop TM-1000 SEM microscope.....	44
Fig. 29: Newtonian viscosity, η_0 , for virgin and degraded PPs obtained from shear creep measurements at 180 °C.....	45
Fig. 30: Reduced steady-state uniaxial extensional viscosity, η_E/a_T , data at 180 °C normalized by the three-fold Newtonian viscosity, $3\eta_0$, for virgin and thermally degraded branched PPs plotted as the function of reduced extensional strain rate, $a_T \dot{\epsilon}$. Here a_T stands for the horizontal Arrhenius shift factor	46
Fig. 31: Simplified visualization of possible changes in “characteristic” polymer coil for investigated branched PP (Daploy WB180HMS) at 180 °C during thermal degradation	48
Fig. 32: Deformation rate dependent shear viscosity data for linear isotactic PP Borflow 64k at 230 °C	49
Fig. 33: Comparison between experimentally determined shear viscosity data and predictions of original (left) and modified Carreau model (right) for linear isotactic PP Borflow 64k sample at 230 °C and fixed η_0 and η_∞ parameters.....	49
Fig. 34: Effect of weight average molecular weight, M_w , and temperature on zero shear viscosity, η_0 , and secondary Newtonian viscosity, η_∞ for L-PP/LCB-PP blends (top) and L-PP (bottom).....	51
Fig. 35: Deformation rate dependent shear viscosity for LCB-PP blend and L-PP having the same molecular weight (64 kg/mol) and polydispersity index (about 4.3) at 230 °C. The term "Corrected" utilized here for shear viscosity and shear rate means that Bagley as well as Weissenberg-Rabinowitsch corrections were applied.....	52
Fig. 36: SEM images for LCB-PP sample and DCD = 500 mm at two different areas and different magnifications (left – 500×, middle – 1000×, right – 2500×) together with corresponding final overall fiber diameter distribution	54
Fig. 37: Effect of η_0/η_∞ on coefficient of fiber diameter variation, CV	55

LIST OF TABLES

<i>Table 1. Summarization of the most important MB die designs in chronological order [5, 15, 16].....</i>	<i>12</i>
<i>Table 2. Typical polymers utilized in the MB technology [1, 20]</i>	<i>15</i>
<i>Table 3. Summarization of products, which can be produced by the MB technology [1] (adapted from [21]).....</i>	<i>16</i>
<i>Table 4. Effect of MB process variables on mean fiber diameter (adapted from [1] and upgraded based on the recent open literature)</i>	<i>19</i>
<i>Table 5. Effect of MB process variables on basic nonwoven characteristics (adapted from [1] and upgraded based on the recent open literature). 20</i>	
<i>Table 6. Basic characteristics for chosen PPs (pellets).....</i>	<i>36</i>

LIST OF PUBLICATIONS

Impact Factor Journal Papers Abstracted on Web of Science Database

1. DRABEK, J. M. ZATLOUKAL, Influence of long chain branching on fiber diameter distribution for polypropylene nonwovens. Submitted for publication in *Journal of Rheology*. 2018. AIS (2017) = 1.129
2. DRABEK, J., M. ZATLOUKAL and M. MARTYN, Effect of molecular weight, branching and temperature on dynamics of polypropylene melts at very high shear rates. *Polymer*. 2018, vol. 144, pp. 179–183. AIS (2017) = 0.740
3. DRABEK, J., M. ZATLOUKAL and M. MARTYN, Effect of molecular weight on secondary Newtonian plateau at high shear rates for linear isotactic melt blown polypropylenes. *Journal of Non-Newtonian Fluid Mechanics*. 2018, vol. 251, pp. 107–118. AIS (2017) = 0.769
4. DRABEK, J., M. ZATLOUKAL, Evaluation of thermally induced degradation of branched polypropylene by using rheology and different constitutive equations. *Polymers*. 2016, Vol. 8, Issue 9, article n. 317. AIS (2016) = 0.941

Conference Papers Abstracted on Web of Science and/or Scopus Database

1. ZATLOUKAL, M., J. DRABEK and M. MARTYN, Measurement and modeling of flow behaviour for melt blown polymer melt in very wide deformation rate range. *Annual Technical Conference – ANTEC, Conference Proceedings*. 2017, pp. 233–238. ISBN 978-0-692-88309-9.
2. DRABEK, J., M. ZATLOUKAL and M. MARTYN, Investigation of flow behavior for linear melt blown polypropylenes with different molecular weights in very wide shear rate range. *AIP Conference Proceedings*. 2017, vol. 1843, pp. 030007-1–030007-11. ISBN 978-073541513-3.

3. ZATLOUKAL, M., J. DRABEK, Evaluation of branched polypropylene degradation by using different constitutive equations. *Annual Technical Conference – ANTEC, Conference Proceedings*. 2016, pp. 117–122. ISBN 978-069271961-9.
4. DRABEK, J., M. ZATLOUKAL, Investigation of thermal degradation of branched polypropylene via rheology. *AIP Conference Proceedings*. 2015, vol. 1662, pp. 030008-1 – 030008-7. ISBN 978-073541306-1.
5. DRABEK, J., M. ZATLOUKAL, Rheological evaluation of melt blown polymer. *AIP Conference Proceedings*. 2013, vol. 1526, pp. 237–247. ISBN 978-073541151-7.

Conference Contributions

1. ZATLOUKAL, M., J. DRABEK, M. MARTYN, Effect of molecular weight on dynamics of linear isotactic polypropylene melt at very high shear rates. *ANTEC[®] 2018 – Orlando, Florida, USA May 7–10, 2018*. [On-line]. Society of Plastics Engineers.
2. DRABEK, J., M. ZATLOUKAL, M. MARTYN, High shear rate rheology of branched polypropylenes. *POLYMERS: Site of Advanced Horizons and Ambits*. 2018, P-07. ISBN 978-80-7454-729-4.
3. DRABEK, J., M. ZATLOUKAL, Applied rheology for production of polymeric nanofibers by melt blown technology. *Czech Chem. Soc. Symp. Ser.* 2018, 11L-05, p. 450. ISSN 2336-7202.

CURRICULUM VITAE

Personal information

First name / Surname	Jiří Drábek, Ing., Bc.
Address	Tomas Bata University in Zlín, Faculty of Technology, Polymer Centre, Vavrečkova 275, Zlín 760 01 Czech Republic
Telephone	+420 57 603 1422
E-mail	jdrabek89@seznam.cz
Nationality	Czech
Date of birth	5.5. 1989
Birthplace	Zlín, Czech Republic

Education

Period	2013 – present
Title of qualification awarded	Ph.D.
Principal branch	Technology of Macromolecular Compounds
Organisation providing education	Tomas Bata University in Zlín, Faculty of Technology Polymer Centre
Period	2013 - 2015
Title of qualification awarded	Bc.
Principal branch	Secondary School Teacher Training in Specialized Subjects
Organisation providing education	Tomas Bata University in Zlín, Faculty of Humanities Department of School Education
Period	2011 – 2013
Title of qualification awarded	Ing.
Principal branch	Technological Equipments Design
Organisation providing education	Tomas Bata University in Zlín, Faculty of Technology, Department of Production Engineering
Period	2008 – 2011
Title of qualification awarded	Bc.
Principal branch	Technological Equipments
Organisation providing education	Tomas Bata University in Zlín, Faculty of Technology, Department of Production Engineering
Period	2004 – 2008
Principal branch	Electronics Mechanic
Organisation providing education	Secondary Technical Polytechnic School, Training center Zlín

Training Abroad

Date	2016 (8 months)
Place	Great Britain, West Yorkshire, Bradford
Organisation providing training	University of Bradford, IRC in Polymer Science and Technology School of Engineering

Awards

2016	Best Paper Award Evaluation of Branched Polypropylene Degradation by Using Different Constitutive Equations Society of Plastic Engineers (SPE), Applied Rheology Division ANTEC 2016 conference in Indianapolis, Indiana, USA
2013	Award by the Dean of the Faculty of Technology of TBU in Zlin

Conferences

2011, 2013, 2015, 2017	Novel Trends in Rheology IV, V, VI, VII International conferences held by Tomas Bata University Member of organization team
------------------------	---

Work on projects

2016 – present	Grant GAČR 16-05886S <i>Investigation the Effect of Polymer Melt Shear and Elongational Rheology on Production Stability of Meltblown Nanofibers and Films</i> Member of research team
2016	Grant UTB IGA/FT/2016/007 <i>Modelling of free surface viscoelastic melt flow</i> Member of research team
2015	Grant UTB IGA/FT/2015/013 <i>Investigation of melt flow stability in flat film production</i> Member of research team
2012 – 2014	Grant GAČR P108/10/1325 <i>Applied Rheology for Advanced Polymer Processing</i> Member of research team

Ing. Bc. Jiří Drábek, Ph.D.

Applied Rheology for Production of Polymeric Nanofibers

Aplikovaná reologie pro výrobu polymerních nanovláken

Doctoral Thesis Summary

Published by: Tomas Bata University in Zlín,
nám. T. G. Masaryka 5555, 760 01 Zlín.

Edition: published electronically

Typesetting by: Ing. Bc. Jiří Drábek, Ph.D.

This publication has not undergone any proofreading or editorial review.

Publication year: 2018

First Edition

ISBN 978-80-7454-819-2